REPORT No. 716

A SIMPLIFIED THEORETICAL METHOD OF DETERMINING THE CHARACTERISTICS OF A LIFTING ROTOR IN FORWARD FLIGHT

By F. J. Bailey, Jr.

SUMMARY

Theoretically derived expressions for the flapping, the thrust, the torque, and the profile drag-lift ratio of a nonfeathering rotor with hinged, rectangular, linearly twisted blades are given as simple functions of the inflow velocity and the blade pitch. Representative values of the coefficients of each of the terms in these expressions are tabulated for a series of specified values of the tip-speed ratio. Analysis indicates that the tabulated values can be used to calculate, with reasonable accuracy, the characteristics of any rotor of conventional design.

In order to demonstrate the method of using the tables included with the analysis, the characteristics of a typical autorotating rotor are calculated. A convenient method is devised for expressing, by means of a single chart, the relationship between the drag and the lift characteristics of the rotor for various combinations of pitch, tip-speed ratio, and solidity.

The decelerating torque and the profile drag-lift ratio of the rotor are evaluated on the assumption that the profile-drag coefficient of a blade element can be expressed as a function of the angle of attack of the element by the first three terms of a power series. A convenient method is developed for determining appropriate values of the coefficients of the different powers of the angle of attack in this series for conventional airfoil sections at any Reynolds number.

When the blade elements reach angles of attack above a certain limiting value, the drag coefficient begins to exceed the value given by the series. For certain limiting conditions of pitch and tip-speed ratio, where the elements begin to reach high angles while moving at high velocity, the rotor performance is impaired and the theory becomes optimistic. A method of determining these limiting conditions is developed.

A further limitation, imposed by the requirement that compressibility shock be avoided at the advancing blade tip, is found to limit high-speed flight to high tip-speed ratios, where the autorotating rotor is inherently inefficient.

INTRODUCTION

Theoretical expressions from which the various characteristics of autogiro and helicopter rotors can be calculated are to be found in the works of Wheatley (references 1 and 2) and Sissingh (reference 3). The form in which these expressions have been presented is unsatisfactory for practical engineering calculations, chiefly because the expressions have not been reduced to terms of the two basic parameters: inflow velocity and blade pitch.

In the present paper the theoretical expressions for thrust coefficient, flapping coefficient, accelerating torque coefficient, decelerating torque coefficient, and profile drag-lift ratio are reduced to simple functions of the inflow factor λ and the blade pitch angles θ_0 and θ_1. The coefficients of the various terms in the expressions are found to be functions of the tip-speed ratio μ, the mass constant γ, and the tip-loss factor B. Values of these coefficients, computed for $\gamma=15$ and $B=0.97$, have been tabulated for a series of specified values of the tip-speed ratio. Because the departures of γ from 15 and B from 0.97 that are to be expected in modern rotor designs have a negligible effect on the values of the coefficients, the tabulated values can be safely used for calculating the characteristics of any conventional rotor.

In the derivation of expressions for the decelerating torque and the profile drag-lift ratio, it is necessary to approximate the relation between the section profile-drag coefficient c_{d_0} and the angle of attack α_r of a blade element. This approximation is made in the present paper by means of the power series:

$$c_{d_0}=\delta_0+\delta_1\alpha_r+\delta_2\alpha_r^2$$

From the data of reference 4, a convenient method is then developed for assigning appropriate values to the coefficients δ_0, δ_1, and δ_2 for conventional airfoil sections at any Reynolds number.

When blade elements approach or exceed the stall, their drag coefficients greatly exceed the values given by this approximation. At the same time their lift coefficients fall below the values given by the approximation

$$c_l=a\alpha_r$$

that is used to express the relation between the lift coefficient and the angle of attack of an element. As long as such elements are confined to parts of the rotor where the relative velocity between the air and the elements is low, the contribution of these elements

to the total rotor force is small and the theory is accurate. When the conditions of pitch and tip-speed ratio exceed certain limits, however, blade elements begin to operate near or beyond the stall while moving at high velocities. Their drag then begins to impair the performance of the rotor and the theory becomes optimistic. In order to prevent the unwitting application of the theory to these conditions, in which its basic assumptions are untenable, a method of determining approximately the limiting combinations of pitch and tip-speed ratio is presented.

A source of much confusion in the analysis of data on rotor drag has been the lack of a method of presenting the data in a simple form capable of showing directly and independently the effects of changes in the pitch, the tip-speed ratio, and the solidity. It is shown in the present paper that a chart of the profile drag-lift ratio against the lift coefficient-solidity ratio C_L/σ for a series of specified values of pitch and tip-speed ratios completely satisfies the requirements.

Calculations of the speed of the tip of the advancing blade are included to show that, if compressibility shock is to be avoided at this point, high translational speeds are feasible only at high tip-speed ratios. An autorotating rotor becomes inefficient at these high tip-speed ratios because of the stalling of the retreating blade.

The method of using all the tables and charts included in this paper is fully explained and illustrated by sample calculations for a typical rotor.

The scope of the paper is limited to linearly twisted, rectangular blades with the flapping hinge perpendicular to the rotor axis and to the blade span. Periodic blade-twist terms are not included in view of the current trend toward blades designed to eliminate periodic twist. In the derivation of all the expressions that are functions of the tip-speed ratio μ, all terms of the order of μ^4 or lower have been retained and all terms of the order of μ^5 or higher have been dropped.

SYMBOLS

Ω	rotor angular velocity, radians per second
R	blade radius
V	forward speed
$\lambda\Omega R$	speed of axial flow through rotor
μ	tip-speed ratio ($V\cos\alpha/\Omega R$)
$\mu\Omega R$	component of forward speed in plane of disk
B	tip loss factor Blade elements outboard of radius BR are assumed to have drag but no lift.
r	radius of blade element
x	ratio of blade-element radius to rotor-blade radius (r/R)
$u_T\Omega R$	velocity component at blade element perpendicular to blade span and parallel to rotor disk
b	number of blades
c	blade chord
$u_P\Omega R$	velocity component at blade element perpendicular both to blade span and to $u_T\Omega R$
θ_0	blade pitch angle at hub, radians
θ_1	difference between hub and tip pitch angles, radians
a	slope of lift coefficient against angle of attack of blade airfoil section (radian measure)
σ	solidity, ratio of total blade area to swept-disk area ($bc/\pi R$)
ρ	air density
I_1	mass moment of inertia of rotor blade about horizontal hinge
γ	mass constant of rotor blade ($c\rho aR^4/I_1$)
M_W	weight moment of blade about horizontal hinge
T	rotor thrust
$C_T=$	$T/\rho\Omega^2\pi R^4$
Q	rotor torque
$C_Q=$	$Q/\rho\Omega^2\pi R^5$
L	rotor lift
$C_L=$	$L/\frac{1}{2}\rho V^2\pi R^2$
D	rotor drag
$C_D=$	$D/\frac{1}{2}\rho V^2\pi R^2$
α	angle of attack of rotor disk
α_r	angle of attack of blade element
β	blade flapping angle
ψ	blade azimuth angle (measured from downwind position in direction of rotation)
c_{d_0}	section profile-drag coefficient of a blade element operating normally
c_{d_0}'	section profile-drag coefficient of a blade element in reversed-velocity region
$\delta_0, \delta_1, \delta_2$	coefficients in power series expressing c_{d_0} as a function of c_l
c_l	section lift coefficient of a blade element
a_0	constant term in Fourier series that expresses β
a_n	coefficient of $\cos n\psi$ in expression for β
b_n	coefficient of $\sin n\psi$ in expression for β

ANALYSIS

FLAPPING COEFFICIENTS

The flapping angle β between the blade-span axis and the plane perpendicular to the rotor axis is a function of the azimuth position of the blade. The relation between β and the azimuth angle ψ of the blade can be approximated with sufficient accuracy by the Fourier series.

$$\beta=a_0-a_1\cos\psi-b_1\sin\psi-a_2\cos 2\psi-b_2\sin 2\psi$$

Expressions for the flapping coefficients a_0, a_1, and b_1 are given in equations (9) to (11) of reference 1. By substitution and division these expressions can be reduced to the form:

$$\frac{a_0}{\gamma}=(t_{1,1})\lambda+(t_{1,2})\theta_0+(t_{1,3})\theta_1-\frac{1}{\gamma}\frac{M_W}{I_1\Omega^2} \quad (1)$$

$$a_1=(t_{1,4})\lambda+(t_{1,5})\theta_0+(t_{1,6})\theta_1 \quad (2)$$

$$\frac{b_1}{\gamma}=(t_{1,7})\lambda+(t_{1,8})\theta_0+(t_{1,9})\theta_1+(t_{1,10})\frac{1}{\gamma}\frac{M_W}{I_1\Omega^2} \quad (3)$$

where the symbols $(t_{1,1})$, $(t_{1,2})$, etc. are used to represent lengthy expressions involving the tip-speed ratio μ, the tip-loss factor B, and the blade mass constant γ. The actual expressions represented are given in full in the appendix.

In equations (1), (2), and (3) the coefficients of λ, θ_0, θ_1, and $\frac{1}{\gamma}\frac{M_W}{I_1\Omega^2}$ are, for all practical purposes, independent of γ for values of μ up to 0.5 and for values of γ up to 25. For example, at a tip-speed ratio of 0.5, reducing γ from 15 to 0 changes no coefficient by more than 2.9 percent. Increasing γ from 15 to 25 changes no coefficient by more than 1.3 percent. All terms that involve γ are of the order of μ^3 or μ^4; hence, the effect of γ decreases very rapidly as the tip-speed ratio is reduced.

Numerical values of the coefficients of λ, θ_0, θ_1, and $\frac{1}{\gamma}\frac{M_W}{I_1\Omega^2}$ in equations (1), (2), and (3) are given for specified tip-speed ratios in table I. The values given have been computed on the assumption that the mass constant γ is 15 but these values may be used, with satisfactory accuracy, for any value of γ from 0 to 25. It will be noted that the subscripts of the symbols $(t_{1,1})$, $(t_{1,2})$, etc. used in the equations have been chosen to indicate the table and the line in that table where the appropriate numerical values are to be found. This procedure is followed throughout the paper.

TABLE I.—NUMERICAL VALUES OF THE COEFFICIENTS IN EQUATIONS (1), (2), AND (3)

[$\gamma=15$; $B=0.97$]

Coefficient of \ Tip-speed ratio, μ	0.15	0.20	0.25	0.30	0.35	0.40	0.45	0.50
				a_0/γ in equation (1)				
λ	0.1523	0.1525	0.1527	0.1531	0.1536	0.1543	0.1550	0.1560
θ_0	.1133	.1153	.1178	.1209	.1244	.1284	.1328	.1375
θ_1	.0877	.0890	.0906	.0927	.0950	.0977	.1006	.1038
				a_1 in equation (2)				
λ	0.322	0.431	0.543	0.659	0.777	0.899	1.026	1.159
θ_0	.418	.564	.715	.874	1.041	1.217	1.405	1.607
θ_1	.304	.410	.520	.634	.755	.881	1.016	1.159
				b_1/γ in equation (3)				
λ	0.0313	0.0415	0.0517	0.0619	0.0721	0.0822	0.0925	0.1028
θ_0	.0233	.0315	.0401	.0493	.0591	.0696	.0809	.0933
θ_1	.0180	.0242	.0308	.0377	.0449	.0526	.0609	.0697
$\frac{1}{\gamma}\frac{M_W}{I_1\Omega^2}$	−.204	−.269	−.334	−.393	−.452	−.507	−.557	−.606

In table I, and in all subsequent computations in the present paper, the effective blade radius is assumed to be 97 percent of the actual radius; that is, the tip-loss factor B is 0.97. For conventional rotor-blade designs this value is considered to be a sufficiently close approximation to the recommended value $1-c/2R$ (reference 1).

Expressions for the flapping coefficients a_2 and b_2 are given in equations (9 15) of reference 1. These expressions can be written in the form:

$$\frac{a_2}{\mu^2}=(t_{2,1})\lambda+(t_{2,2})\theta_0+(t_{2,3})\theta_1 \tag{4}$$

$$\frac{b_2}{\mu^2}=(t_{2,4})\lambda+(t_{2,5})\theta_0+(t_{2,6})\theta_1 \tag{5}$$

The coefficients of λ, θ_0, and θ_1 in equations (4) and (5) are not independent of γ but are independent of μ. Values of these coefficients for specified values of γ are given in table II. Complete expressions for each coefficient are given in the appendix.

TABLE II. NUMERICAL VALUES OF THE COEFFICIENTS IN EQUATIONS (4) AND (5)

[$B=0.97$]

Coefficient of \ Mass constant, γ	0	2	4	6	8	10	12	14	16	18	20
					a_2/μ^2 in equation (4)						
λ	0	0.214	0.417	.602	.769	.919	1.056	1.184	1.306	1.423	1.539
θ_0	0	.198	.383	.548	.689	.810	.915	1.009	1.096	1.177	1.257
θ_1	0	.150	.291	.417	.525	.618	.699	.772	.839	.903	.965
					b_2/μ^2 in equation (5)						
λ	0	−0.013	−0.049	−0.100	−0.157	−0.214	−0.268	−0.314	−0.354	−0.388	−0.417
θ_0	0	−.016	−.059	−.121	−.191	−.260	−.324	−.381	−.430	−.471	−.506
θ_1	0	−.012	−.044	−.090	−.142	−.194	−.242	−.284	−.320	−.351	−.377

THRUST COEFFICIENT

The expression for the thrust coefficient given in equation (8–14) of reference 1 can, after substitution from equations (2) and (5), be reduced to the form

$$\frac{2C_T}{\sigma a}=(t_{3,1})\lambda+(t_{3,2})\theta_0+(t_{3,3})\theta_1 \tag{6}$$

Again the coefficients of λ, θ_0, and θ_1 are practically independent of γ. At a tip-speed ratio of 0.5, a reduction of γ from 15 to 0 changes no coefficient by more than 1.7 percent while an increase in γ from 15 to 25 changes no coefficient by more than 0.7 percent.

Numerical values of these coefficients, computed for $\gamma=15$ but satisfactory for any value of γ between 0 and 25, are given in table III. Complete expressions for each coefficient are given in the appendix.

TABLE III.—NUMERICAL VALUES OF THE COEFFICIENTS IN EQUATION (6) FOR $2C_T/\sigma a$

[$\gamma=15$; $B=0.97$]

Coefficient of \ Tip-speed ratio, μ	0.15	0.20	0.25	0.30	0.35	0.40	0.45	0.50
λ	0.476	0.480	0.487	0.494	0.504	0.515	0.529	0.544
θ_0	.315	.322	.333	.346	.361	.379	.399	.422
θ_1	.226	.230	.237	.243	.252	.263	.275	.289

ANGLE OF ATTACK

After the thrust coefficient C_T has been determined, the angle of attack α between the plane perpendicular to the rotor axis and the flight path can be obtained from equation (5–2) of reference 1, which is

$$\tan\alpha=\frac{\lambda}{\mu}+\frac{C_T}{2\mu(\lambda^2+\mu^2)^{1/2}} \tag{7}$$

For low angles of attack λ^2 is negligible in comparison with μ^2 and the expression reduces to

$$\alpha=\frac{\lambda}{\mu}+\frac{C_T}{2\mu^2} \tag{8}$$

ACCELERATING TORQUE

In previous work on the torque equilibrium of autogiro rotors (reference 5), it was found convenient to divide the aerodynamic torque into two parts: one dependent on the components of the lift vectors of the blade elements parallel to the plane of the disk and the other dependent on the components of the drag vectors parallel to the plane of the disk. In the case of the autogiro, the torque arising from the inclination of the lift vectors relative to the plane of the disk tends to accelerate the rotor and was designated the accelerating torque in reference 5. This designation will be retained in the present paper even though, in the case of the helicopter, the inclination of the elemental lift vectors may tend to decelerate the rotor.

A study of equation (9) of reference 5 shows that the accelerating torque coefficient C_{Q_a} of a rotor without dynamic blade twist can be expressed in the form

$$\begin{aligned}\frac{1}{a}\left(\frac{2C_{Q_a}}{\sigma}\right)&=(t_{4,1})\lambda^2+(t_{4,2})\lambda\theta_0+(t_{4,3})\lambda\theta_1+(t_{4,4})\theta_0^2\\&+(t_{4,5})\theta_0\theta_1+(t_{4,6})\theta_1^2+(t_{4,7})\gamma\frac{M_W}{I_1\Omega^2}\lambda+(t_{4,8})\gamma\frac{M_W}{I_1\Omega^2}\theta_0\\&+(t_{4,9})\gamma\frac{M_W}{I_1\Omega^2}\theta_1+(t_{4,10})\left(\frac{M_W}{I_1\Omega^2}\right)^2\end{aligned} \tag{9}$$

The expressions represented by the symbols $(t_{4,1})$, $(t_{4,2})$, etc. are given in the appendix.

The last four terms of equation (9) are negligible for combinations of γ and $M_W/I_1\Omega^2$ found in current autogiro designs.

Numerical values of the coefficients in the first six terms, computed for $\gamma=15$, are included in table I of reference 5. For convenience these values are repeated in table IV in the present paper. Reasonable departures of the mass constant γ from 15 can again be safely ignored although the effect of changes in γ is somewhat greater than it was in the case of thrust and flapping. At $\mu=0.5$ the maximum change produced in any of the coefficients by decreasing γ from 15 to 0 is 5.6 percent and the maximum change produced by increasing γ from 15 to 25 is 9.2 percent.

TABLE IV.—NUMERICAL VALUES OF THE COEFFICIENTS IN EQUATION (9) FOR $1/a$ $(2C_{Q_a}/\sigma)$

[$\gamma=15$; $B=0.97$]

Coefficient of \ Tip-speed ratio, μ	0.15	0.20	0.25	0.30	0.35	0.40	0.45	0.50
λ^2	0.502	0.526	0.558	0.598	0.646	0.702	0.766	0.840
$\lambda\theta_0$	.369	.421	.490	.579	.689	.824	.986	1.179
$\lambda\theta_1$	.268	.306	.356	.420	.500	.598	.714	.854
θ_0^2	.022	.040	.066	.100	.145	.203	.276	.368
$\theta_0\theta_1$	.032	.058	.096	.146	.212	.296	.403	.536
θ_1^2	.012	.021	.035	.053	.077	.108	.147	.195

A comparison of the expression for the accelerating torque of a constant-pitch rotor of pitch $\theta_0+\Delta\theta_0$ with that for a rotor of pitch θ_0 and linear twist θ_1 shows that the two rotors will have the same accelerating torque at the same inflow factor if

$$\Delta\theta_0=\frac{(t_{4,3})}{(t_{4,2})}\theta_1=\frac{(t_{4,5})}{2(t_{4,4})}\theta_1=\sqrt{\frac{(t_{4,6})}{(t_{4,4})}}\theta_1$$

A study of the numerical values given in table IV shows that, for all practical purposes,

$$\frac{(t_{4,3})}{(t_{4,2})}=\frac{(t_{4,5})}{2(t_{4,4})}=\sqrt{\frac{(t_{4,6})}{(t_{4,4})}}=\frac{3}{4}B$$

Hence the accelerating torque of a rotor with linearly twisted blades is, for practical purposes, equivalent to that of a constant-pitch rotor if the pitch of the elements at 75 percent of the effective radius BR is identical in the two rotors. Considerable time can be saved in calculating the accelerating torque of a rotor with linearly twisted blades by first determining the blade pitch at $0.75BR$ and then calculating the torque of a rotor with untwisted blades having this pitch.

DECELERATING TORQUE

The decelerating torque coefficient C_{Q_d} of the rotor can be expressed in the integral form by following the method developed in reference 1:

$$\begin{aligned}\left(\frac{2C_{Q_d}}{\sigma}\right)=&\frac{1}{2\pi}\int_0^{\pi}d\psi\int_0^1 u_T{}^2c_{d_0}x\,dx\\&+\frac{1}{2\pi}\int_{\pi}^{2\pi}d\psi\int_{-\mu\sin\psi}^1 u_T{}^2c_{d_0}x\,dx\\&-\frac{1}{2\pi}\int_{\pi}^{2\pi}d\psi\int_0^{-\mu\sin\psi}u_T{}^2c_{d_0}{}'x\,dx\end{aligned}\qquad(10)$$

In this expression, c_{d_0} represents the profile-drag coefficient of a blade element operating normally and $c_{d_0}{}'$ represents the profile-drag coefficient of an element in the reversed-velocity region.

Experience has shown that the drag coefficient of a blade element cannot be considered to be independent of ψ and x; hence equation (10) cannot be integrated until c_{d_0} and $c_{d_0}{}'$ are expressed in terms of ψ and x. The simplest way of satisfying this requirement is to approximate the relation between the drag coefficient and the angle of attack of an element by a power series of the form

$$c_{d_0}=\delta_0+\delta_1\alpha_r+\delta_2\alpha_r{}^2=\delta_0+\delta_1\left(\frac{u_P}{u_T}+\theta_0+x\theta_1\right)+\delta_2\left(\frac{u_P}{u_T}+\theta_0+x\theta_1\right)^2$$

as was originally done by Sissingh in reference 3.

The effective angle of attack of elements in the reversed-velocity region has been shown in reference 1 to be

$$\alpha_r{}'=-\frac{u_P}{u_T}-\theta_0-x\theta_1$$

It will therefore be assumed that

$$c_{d_0}{}'=\delta_0+\delta_1\left(-\frac{u_P}{u_T}-\theta_0-x\theta_1\right)+\delta_2\left(-\frac{u_P}{u_T}-\theta_0-x\theta_1\right)^2$$

With ordinary airfoil sections, of course, the values of δ_0, δ_1, and δ_2 appropriate for backward-moving blade elements in the reversed-velocity region may be expected to differ considerably from the values characteristic of the forward-moving elements in the rest of the disk. At tip-speed ratios below 0.5, however, the total contribution of the reversed-velocity region is too small to necessitate any such refinement in its evaluation.

After substitution for c_{d_0} and $c_{d_0}{}'$ equation (10) becomes

$$\begin{aligned}\left(\frac{2C_{Q_d}}{\sigma}\right)=&\delta_0\left[\frac{1}{2\pi}\int_0^{\pi}d\psi\int_0^1 u_T{}^2x\,dx+\frac{1}{2\pi}\int_{\pi}^{2\pi}d\psi\int_{-\mu\sin\psi}^1 u_T{}^2x\,dx\right.\\&\left.-\frac{1}{2\pi}\int_{\pi}^{2\pi}d\psi\int_0^{-\mu\sin\psi}u_T{}^2x\,dx\right]\\&+\delta_1\left[\frac{1}{2\pi}\int_0^{\pi}d\psi\int_0^1 u_T{}^2\left(\frac{u_P}{u_T}+\theta_0+x\theta_1\right)x\,dx\right.\\&+\frac{1}{2\pi}\int_{\pi}^{2\pi}d\psi\int_{-\mu\sin\psi}^1 u_T{}^2\left(\frac{u_P}{u_T}+\theta_0+x\theta_1\right)x\,dx\\&\left.-\frac{1}{2\pi}\int_{\pi}^{2\pi}d\psi\int_0^{-\mu\sin\psi}u_T{}^2\left(-\frac{u_P}{u_T}-\theta_0-x\theta_1\right)x\,dx\right]\\&+\delta_2\left[\frac{1}{2\pi}\int_0^{\pi}d\psi\int_0^1 u_T{}^2\left(\frac{u_P}{u_T}+\theta_0+x\theta_1\right)^2x\,dx\right.\\&+\frac{1}{2\pi}\int_{\pi}^{2\pi}d\psi\int_{-\mu\sin\psi}^1 u_T{}^2\left(\frac{u_P}{u_T}+\theta_0+x\theta_1\right)^2x\,dx\\&\left.-\frac{1}{2\pi}\int_{\pi}^{2\pi}d\psi\int_0^{-\mu\sin\psi}u_T{}^2\left(-\frac{u_P}{u_T}-\theta_0-x\theta_1\right)^2x\,dx\right]\end{aligned}$$

which reduces to

$$\begin{aligned}\left(\frac{2C_{Q_d}}{\sigma}\right)=&\delta_0\left[\frac{1}{2\pi}\int_0^{2\pi}d\psi\int_0^1 u_T{}^2x\,dx-\frac{1}{\pi}\int_{\pi}^{2\pi}d\psi\int_0^{-\mu\sin\psi}u_T{}^2x\,dx\right]\\&+\delta_1\left[\frac{1}{2\pi}\int_0^{2\pi}d\psi\int_0^1 u_T{}^2\left(\frac{u_P}{u_T}+\theta_0+x\theta_1\right)x\,dx\right]\\&+\delta_2\left[\frac{1}{2\pi}\int_0^{2\pi}d\psi\int_0^1 u_T{}^2\left(\frac{u_P}{u_T}+\theta_0+x\theta_1\right)^2x\,dx\right.\\&\left.-\frac{1}{\pi}\int_{\pi}^{2\pi}d\psi\int_0^{-\mu\sin\psi}u_T{}^2\left(\frac{u_P}{u_T}+\theta_0+x\theta_1\right)^2x\,dx\right]\end{aligned}$$

After substitution for u_T and u_P from equations (8), (9), (10), and (11) of reference 2, integration, and substitution for the flapping coefficients from equations (1) to (5) of this report, the expression for decelerating torque takes the form

$$\begin{aligned}\left(\frac{2C_{Q_d}}{\sigma}\right)=&\delta_0(t_{5,1})+\delta_1\left[(t_{5,2})\lambda+(t_{5,3})\theta_0+(t_{5,4})\theta_1\right]\\&+\delta_2\left[(t_{5,5})\lambda^2+(t_{5,6})\lambda\theta_0+(t_{5,7})\lambda\theta_1+(t_{5,8})\theta_0{}^2\right.\\&+(t_{5,9})\theta_0\theta_1+(t_{5,10})\theta_1{}^2\\&+(t_{5,11})\gamma\frac{M_W}{I_1\Omega^2}\lambda+(t_{5,12})\gamma\frac{M_W}{I_1\Omega^2}\theta_0+(t_{5,13})\gamma\frac{M_W}{I_1\Omega^2}\theta_1\\&\left.+(t_{5,14})\left(\frac{M_W}{I_1\Omega^2}\right)^2\right]\end{aligned}\qquad(11)$$

The complete expressions for the coefficients represented by the symbols $(t_{5,1})$, $(t_{5,2})$, etc. are given in the appendix.

The net contribution of the last four terms in equation (11), that is, the terms containing $M_W/I_1\Omega^2$, is negligible for normal values of γ and $M_W/I_1\Omega^2$. Values of the coefficients in the first 10 terms are given in table V for $\gamma=15$, $B=0.97$. The effect of γ on the value of these coefficients is again very small. At a tip-speed ratio of 0.5, no coefficient changes by more than than 3.6 percent as γ is reduced from 15 to zero or by more than 4.6 percent as γ is increased from 15 to 25.

TABLE V.—NUMERICAL VALUES OF THE COEFFICIENTS IN EQUATION (11) FOR $(2C_{Q_d}/\sigma)$

[$\gamma=15$; $B=0.97$]

Coefficient of \ Tip-speed ratio, μ	0.15	0.20	0.25	0.30	0.35	0.40	0.45	0.50
δ_0	0.256	0.260	0.266	0.272	0.280	0.289	0.299	0.310
$\delta_1\lambda$	.333	.333	.333	.333	.333	.332	.332	.331
$\delta_1\theta_0$	.256	.260	.265	.272	.280	.289	.298	.309
$\delta_1\theta_1$	.204	.207	.210	.215	.220	.226	.232	.239
$\delta_2\lambda^2$	.535	.562	.597	.641	.694	.756	.829	.912
$\delta_2\lambda\theta_0$	.737	.795	.871	.970	1.092	1.242	1.422	1.637
$\delta_2\lambda\theta_1$	.551	.593	.648	.719	.807	.914	1.043	1.197
$\delta_2\theta_0^2$	.280	.305	.339	.385	.443	.518	.610	.724
$\delta_2\theta_0\theta_1$	.443	.479	.528	.593	.676	.782	.914	1.076
$\delta_2\theta_1^2$	.183	.196	.214	.237	.268	.306	.354	.413

PROFILE DRAG

The profile drag-lift ratio of the rotor can be expressed in the integral form by following the procedure outlined in section 11 of reference 1:

$$\left(\frac{D}{L}\right)_0=\frac{\sigma}{2\mu C_T}\left(\frac{1}{2\pi}\int_0^{\pi}d\psi\int_0^1 u_T{}^3c_{d_0}dx+\frac{1}{2\pi}\int_{\pi}^{2\pi}d\psi\int_{-\mu\sin\psi}^1 u_T{}^3c_{d_0}dx-\frac{1}{2\pi}\int_{\pi}^{2\pi}d\psi\int_0^{-\mu\sin\psi}u_T{}^3c_{d_0}{}'dx\right) \tag{12}$$

Under the same assumptions as to the profile-drag coefficient of a blade element that were used in evaluating the decelerating torque, equation (12) becomes

$$\begin{aligned}\frac{2\mu C_T}{\sigma}\left(\frac{D}{L}\right)_0=&\delta_0\left[\frac{1}{2\pi}\int_0^{\pi}d\psi\int_0^1 u_T{}^3dx+\frac{1}{2\pi}\int_{\pi}^{2\pi}d\psi\int_{-\mu\sin\psi}^1 u_T{}^3dx-\frac{1}{2\pi}\int_{\pi}^{2\pi}d\psi\int_0^{-\mu\sin\psi}u_T{}^3dx\right]\\&+\delta_1\left[\frac{1}{2\pi}\int_0^{\pi}d\psi\int_0^1 u_T{}^3\left(\frac{u_P}{u_T}+\theta_0+x\theta_1\right)dx+\frac{1}{2\pi}\int_{\pi}^{2\pi}d\psi\int_{-\mu\sin\psi}^1 u_T{}^3\left(\frac{u_P}{u_T}+\theta_0+x\theta_1\right)dx\right.\\&\left.-\frac{1}{2\pi}\int_{\pi}^{2\pi}d\psi\int_0^{-\mu\sin\psi}u_T{}^3\left(-\frac{u_P}{u_T}-\theta_0-x\theta_1\right)dx\right]\\&+\delta_2\left[\frac{1}{2\pi}\int_0^{\pi}d\psi\int_0^1 u_T{}^3\left(\frac{u_P}{u_T}+\theta_0+x\theta_1\right)^2dx+\frac{1}{2\pi}\int_{\pi}^{2\pi}d\psi\int_{-\mu\sin\psi}^1 u_T{}^3\left(\frac{u_P}{u_T}+\theta_0+x\theta_1\right)^2dx\right.\\&\left.-\frac{1}{2\pi}\int_{\pi}^{2\pi}d\psi\int_0^{-\mu\sin\psi}u_T{}^3\left(-\frac{u_P}{u_T}-\theta_0-x\theta_1\right)^2dx\right]\end{aligned}$$

which can be reduced to

$$\mu\frac{2C_T}{\sigma a}\left(\frac{D}{L}\right)_0=\frac{\delta_0}{a}\left[\frac{1}{2\pi}\int_0^{2\pi}d\psi\int_0^1 u_T{}^3dx-\frac{1}{\pi}\int_{\pi}^{2\pi}d\psi\int_0^{-\mu\sin\psi}u_T{}^3dx\right]$$

$$\begin{aligned}&+\frac{\delta_1}{a}\left[\frac{1}{2\pi}\int_0^{2\pi}d\psi\int_0^1 u_T{}^3\left(\frac{u_P}{u_T}+\theta_0+x\theta_1\right)dx\right]\\&+\frac{\delta_2}{a}\left[\frac{1}{2\pi}\int_0^{2\pi}d\psi\int_0^1 u_T{}^3\left(\frac{u_P}{u_T}+\theta_0+x\theta_1\right)^2dx\right.\\&\left.-\frac{1}{\pi}\int_{\pi}^{2\pi}d\psi\int_0^{-\mu\sin\psi}u_T{}^3\left(\frac{u_P}{u_T}+\theta_0+x\theta_1\right)^2dx\right]\end{aligned}$$

After substitution for u_T and u_P from equations (8), (9), (10), and (11) of reference 2, integration, and substitution for the flapping coefficients from equations (1) to (5) of this paper, the expression for the profile drag-lift ratio takes the form

$$\begin{aligned}\mu\frac{2C_T}{\sigma a}\left(\frac{D}{L}\right)_0=&\frac{\delta_0}{a}(t_{6,1})+\frac{\delta_1}{a}[(t_{6,2})\lambda+(t_{6,3})\theta_0+(t_{6,4})\theta_1]\\&+\frac{\delta_2}{a}\left[(t_{6,5})\lambda^2+(t_{6,6})\lambda\theta_0+(t_{6,7})\lambda\theta_1+(t_{6,8})\theta_0{}^2\right.\\&+(t_{6,9})\theta_0\theta_1+(t_{6,10})\theta_1{}^2+(t_{6,11})\gamma\frac{M_W}{I_1\Omega^2}\lambda\\&\left.+(t_{6,12})\gamma\frac{M_W}{I_1\Omega^2}\theta_0+(t_{6,13})\gamma\frac{M_W}{I_1\Omega^2}\theta_1+(t_{6,14})\left(\frac{M_W}{I_1\Omega^2}\right)^2\right]\end{aligned} \tag{13}$$

The complete expressions for the coefficients represented by the symbols $(t_{6,1})$, $(t_{6,2})$, etc. are given in the appendix.

The net contribution of the four terms in equation (13) that contain $M_W/I_1\Omega^2$ is negligible for normal values of γ and $M_W/I_1\Omega^2$. Values of the coefficients in the other 10 terms are given in table VI for $\gamma=15$, $B=0.97$. At a tip-speed ratio of 0.5 reducing γ from 15 to zero will change no coefficient by more than 1.3 percent while increasing γ from 15 to 25 will change no coefficient by more than 6.7 percent. Consequently, the values given in the table can be safely used for any conventional rotor.

TABLE VI.—NUMERICAL VALUES OF THE COEFFICIENTS IN EQUATION (13) FOR $\mu\frac{2C_T}{\sigma a}\left(\frac{D}{L}\right)_0$

[$\gamma=15$; $B=0.97$]

Coefficient of \ Tip-speed ratio, μ	0.15	0.20	0.25	0.30	0.35	0.40	0.45	0.50
$\frac{\delta_0}{a}$	0.267	0.280	0.297	0.318	0.343	0.372	0.406	0.443
$\frac{\delta_1}{a}\lambda$	.337	.339	.343	.348	.353	.360	.368	.378
$\frac{\delta_1}{a}\theta_0$	.257	.262	.268	.277	.286	.298	.311	.326
$\frac{\delta_1}{a}\theta_1$	.204	.207	.211	.215	.221	.228	.235	.244
$\frac{\delta_2}{a}\lambda^2$	.522	.540	.562	.592	.627	.671	.722	.781
$\frac{\delta_2}{a}\lambda\theta_0$	.711	.747	.794	.855	.930	1.022	1.134	1.267
$\frac{\delta_2}{a}\lambda\theta_1$	.528	.550	.580	.619	.668	.729	.802	.890
$\frac{\delta_2}{a}\theta_0^2$	.270	.287	.309	.339	.378	.426	.486	.560
$\frac{\delta_2}{a}\theta_0\theta_1$	.427	.449	.479	.518	.568	.632	.710	.805
$\frac{\delta_2}{a}\theta_1^2$	.176	.185	.196	.210	.228	.250	.278	.312

The product $\mu\,2C_T/\sigma a$ on the left-hand side of equation (13) is, from equation (6),

$$\mu\frac{2C_T}{\sigma a}=\left(\frac{1}{2}B^2\mu+\frac{1}{4}\mu^3\right)\lambda+\left(\frac{1}{3}B^3\mu+\frac{1}{2}B\mu^3-\frac{4}{9\pi}\mu^4\right)\theta_0+\left(\frac{1}{4}B^4+\frac{1}{4}B^2\mu^3\right)\theta_1 \tag{14}$$

The coefficients of λ, θ_0, and θ_1, which are independent of γ, are given in table VII for $B=0.97$.

TABLE VII.—NUMERICAL VALUES OF THE COEFFICIENTS IN EQUATION (14) FOR $\mu\frac{2C_T}{\sigma a}$

[$B=0.97$]

Coefficient of \ Tip-speed ratio, μ	0.15	0.20	0.25	0.30	0.35	0.40	0.45	0.50
λ	0.0714	0.0961	0.1215	0.1479	0.1753	0.2042	0.2345	0.2664
θ_0	.0471	.0645	.0831	.1033	.1252	.1491	.1753	.2039
θ_1	.0340	.0462	.0590	.0728	.0876	.1036	.1211	.1401

DETERMINATION OF δ_0, δ_1, AND δ_2

The profile-drag coefficient c_{d_0} has been expressed in terms of the angle of attack of a blade element α_r by the series

$$c_{d_0}=\delta_0+\delta_1\alpha_r+\delta_2\alpha_r^2 \tag{15}$$

where δ_0, δ_1, and δ_2 are constants, so chosen that the series will closely approximate an experimental curve of drag coefficient against angle of attack over the important part of the angle-of-attack range. Obviously the values chosen for δ_0, δ_1, and δ_2 will depend on the airfoil section and the Reynolds number. Hence, if the present paper is to be of any practical value in rotor-performance calculations, a simple and rapid method of determining δ_0, δ_1, and δ_2 for different airfoil sections at any Reynolds number must be developed.

It is shown in reference 4 that the profile-drag coefficient of a conventional airfoil section at any Reynolds number can be expressed as

$$c_{d_0}=c_{d_{0_{min}}}+\Delta c_{d_0} \tag{16}$$

where $c_{d_{0_{min}}}$ depends on the airfoil section and the Reynolds number and the increment Δc_{d_0} depends on the parameter $|c_l-c_{l_{opt}}|/(c_{l_{max}}-c_{l_{opt}})$.

The variation of Δc_{d_0} with $|c_l-c_{l_{opt}}|/(c_{l_{max}}-c_{l_{opt}})$ is expressed graphically in figure 45 of reference 4. Examination of this curve reveals that the series expansion

$$\Delta c_{d_0}=K_0+K_1\left(\frac{|c_l-c_{l_{opt}}|}{c_{l_{max}}-c_{l_{opt}}}\right)+K_2\left(\frac{|c_l-c_{l_{opt}}|}{c_{l_{max}}-c_{l_{opt}}}\right)^2 \tag{17}$$

can be made to approximate very closely the curve over a range of values of $|c_l-c_{l_{opt}}|/(c_{l_{max}}-c_{l_{opt}})$ from 0 to 0.8, provided that the values of K_0, K_1, and K_2 are properly chosen. The nature of the agreement that can be obtained is illustrated in figure 1. In this particular case the following values were used: $K_0=0.0003$, $K_1=-0.0025$, and $K_2=0.0229$. These values were chosen to make the values of Δc_{d_0} given by the series agree with the values given by figure 45 of reference 4 at $|c_l-c_{l_{opt}}|/(c_{l_{max}}-c_{l_{opt}})=0.125$, 0.400, and 0.675.

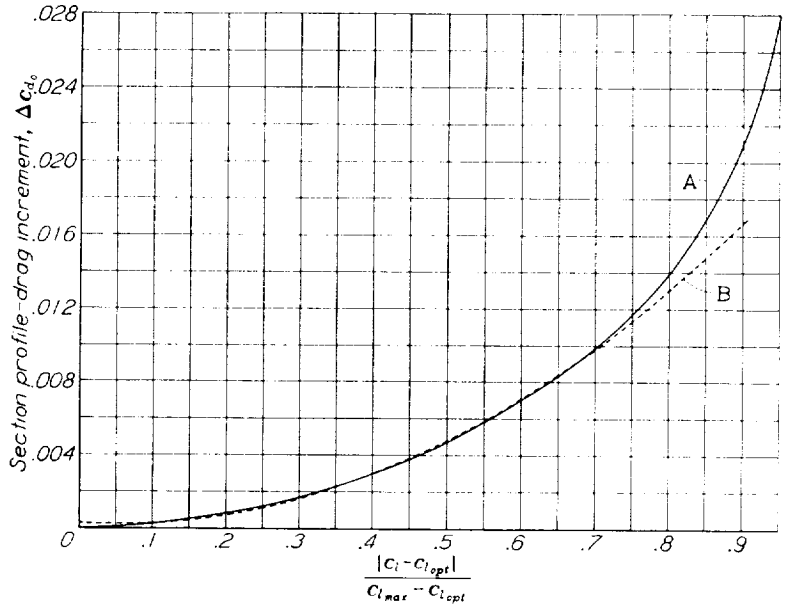

Curve A From figure 45, reference 4

Curve B $\Delta c_{d_0} = 0.0003 - 0.0025\frac{|c_l - c_{l_{opt}}|}{c_{l_{max}} - c_{l_{opt}}} + 0.0229\left(\frac{|c_l - c_{l_{opt}}|}{c_{l_{max}} - c_{l_{opt}}}\right)^2$

FIGURE 1.—Method of approximating profile-drag increment Δc_{d_0} of a blade element.

It will be noted that the substitution of the series for the curve results in some underestimation of the drag of the blade elements operating at very high lift coefficients and some overestimation of the drag at $c_{l_{opt}}$. The overestimation of the drag at $c_{l_{opt}}$ is not considered serious inasmuch as it is to some extent compensated by the slight underestimation of the drag at values of $|c_l - c_{l_{opt}}|/(c_{l_{max}} - c_{l_{opt}})$ from 0.125 to 0.400. In addition, because excessive center-of-pressure travel makes highly cambered sections unsuitable for use in rotors, rotor-blade sections will normally have low values of $c_{l_{opt}}$. For this reason rotor-blade elements will not reach values of c_l as low as $c_{l_{opt}}$ except at the tip of the advancing blade at very high tip-speed ratios.

The underestimation of the drag of elements operating at high angles of attack limits the entire theoretical treatment to those flight conditions in which blade elements do not reach high angles of attack when moving at high velocity relative to the air. Recognition of this limitation is extremely important. If the theory is applied indiscriminately to all flight conditions, absurdly high performance will be predicted at high tip-speed ratios and high pitch settings. This point will be discussed further in connection with an illustrative example in a later section of this paper.

Because values of c_l appreciably below $c_{l_{opt}}$ need not be considered, the algebraic value of $c_l - c_{l_{opt}}$ may be substituted for the absolute value $|c_l - c_{l_{opt}}|$ in equation (17). After the resulting expression for Δc_{d_0} is expanded and the product $a\alpha_r$ is substituted for c_l, it becomes possible, by equating coefficients of like powers of α_r, to express δ_0, δ_1, and δ_2 in the following manner:

$$\delta_0 - c_{d_{0_{min}}} = K_0 - \frac{K_1 c_{l_{opt}}}{c_{l_{max}} - c_{l_{opt}}} + \frac{K_2 c_{l_{opt}}^2}{(c_{l_{max}} - c_{l_{opt}})^2} \quad (18)$$

$$\frac{\delta_1}{a} = \frac{K_1}{c_{l_{max}} - c_{l_{opt}}} - \frac{2K_2 c_{l_{opt}}}{(c_{l_{max}} - c_{l_{opt}})^2} \quad (19)$$

$$\frac{\delta_2}{a^2} = \frac{K_2}{(c_{l_{max}} - c_{l_{opt}})^2} \quad (20)$$

or, when the values chosen for K_0, K_1, and K_2 are incorporated,

$$\delta_0 - c_{d_{0_{min}}} = 0.0003 + 0.0025\frac{c_{l_{opt}}}{c_{l_{max}} - c_{l_{opt}}} + 0.0229\frac{c_{l_{opt}}^2}{(c_{l_{max}} - c_{l_{opt}})^2} \quad (21)$$

$$\frac{\delta_1}{a} = -0.0025\frac{1}{c_{l_{max}} - c_{l_{opt}}} - 0.0458\frac{c_{l_{opt}}}{(c_{l_{max}} - c_{l_{opt}})^2} \quad (22)$$

$$\frac{\delta_2}{a^2} = 0.0229\frac{1}{(c_{l_{max}} - c_{l_{opt}})^2} \quad (23)$$

These expressions are plotted in figure 2 for several values of $c_{l_{opt}}$. Values of δ_0, δ_1, and δ_2 can therefore be directly determined from figures 2(a), 2(b), and 2(c), respectively, for conventional airfoil sections at any Reynolds number if $c_{d_{0_{min}}}$, $c_{l_{max}}$, $c_{l_{opt}}$, and a are known at the Reynolds number in question. Complete directions for determining these last quantities at any desired Reynolds number from standard airfoil tests at some other Reynolds number are given in reference 4.

The variation of the Reynolds number for different parts of the rotor disk complicates the choice of a value on which to base the determination of δ_0, δ_1, and δ_2 for any given rotor. Pending further investigation of this particular problem it is suggested that a value corresponding to the chord and the average rotational speed of the blade element at $0.75R$ be used.

APPLICATION OF THEORY

The manner in which the preceding charts and tables are used will now be illustrated by a numerical evaluation of the characteristics of a particular rotor operating at a specified tip-speed ratio. The rotor used for this example will be assumed to have rectangular blades of the NACA 23012 airfoil section with no linear twist ($\theta_1=0$). The Reynolds number corresponding to the chord and the rotational speed at $0.75R$ will be considered to be approximately 2,000,000. The rotor will be assumed to have a blade pitch angle of 4° and to be autorotating at a tip-speed ratio of 0.35.

For the NACA 23012 airfoil section operating at a Reynolds number of 8,160,000, the following values were obtained from table II of reference 4:

$c_{l_{max}}$	1.72
a, per radian	5.73
$c_{d_{0_{min}}}$	.0070
$c_{l_{opt}}$	.08

Since the publication of table II of reference 4, the data contained therein have been found to be subject to corrections described in reference 6. Table III of reference 6 gives for the NACA 23012 section $c_{l_{max}}=1.74$, $c_{d_{0_{min}}}=0.0060$ at a Reynolds number of 8,400,000. The change in $c_{l_{max}}$ is negligible. The higher value of $c_{d_{0_{min}}}$ used in the present paper may be considered to include a partial allowance for surface roughness. The results published in reference 7 indicate that current construction, for wings at least, is sufficiently crude to increase the minimum profile-drag coefficient by as much as 50 percent over that for a smooth wing.

At a Reynolds number of 2,000,000 a value of $c_{l_{max}}=1.72-0.27=1.45$ is obtained from figure 44 of reference 4. The value of 5.73 for a remains unchanged. The minimum profile-drag coefficient is given by the expression

$$c_{d_{0_{min}}}=\left(c_{d_{0_{min}}}\right)_{std}\left(\frac{R_{std}}{R}\right)^{0.11}$$
$$=(0.0070)\left(\frac{8.16\times10^6}{2\times10^6}\right)^{0.11}$$
$$=0.0082$$

An indication of the probable variation of $c_{l_{opt}}$ with scale for different airfoil sections is given by figure 42 and table I of reference 4. It is to be noted, however, that the accuracy of the experimental data is not sufficient to establish the small variation for the NACA 23012 section with any degree of certainty. For the present example it will be assumed that the effect of scale on $c_{l_{opt}}$ of the NACA 23012 section can be ignored over the range of Reynolds numbers from 8,000,000 to 2,000,000.

The values of δ_0, δ_1, and δ_2 can now be obtained from figure 2 or from equations (21), (22), and (23). They are:

δ_0	0.0087
δ_1	.0216
δ_2	.400

The next step is the determination of the inflow factor λ from the torque equilibrium of the rotor. In the present problem the rotor is assumed to be in steady autorotation; hence, the accelerating and the decelerating torques are exactly equal. That is

$$\left(\frac{2C_{Q_a}}{\sigma}\right)=\left(\frac{2C_{Q_d}}{\sigma}\right)$$

or, at $\mu=0.35$, from equations (9) and (11) and tables IV and V

$$a(0.646\lambda^2+0.689\lambda\theta_0+0.500\lambda\theta_1+0.145\theta_0^2+0.212\theta_0\theta_1$$
$$+0.077\theta_1^2)=0.280\delta_0$$
$$+\delta_1(0.333\lambda+0.280\theta_0+0.220\theta_1)$$
$$+\delta_2(0.694\lambda^2+1.092\lambda\theta_0+0.807\lambda\theta_1+0.443\theta_0^2$$
$$+0.676\theta_0\theta_1+0.268\theta_1^2)$$

Terms involving $M_W/I_1\Omega^2$ have been omitted from this equation on the assumption that $M_W/I_1\Omega^2$ is of normal magnitude (approximately 0.006) so that the net contribution of these terms is negligible.

Substitution of the appropriate values of δ_0, δ_1, δ_2, θ_0, θ_1, and a into the preceding equation gives the quadratic equation

$$3.701\lambda^2+0.2756\lambda+0.004050=0.278\lambda^2+$$
$$0.0233\lambda+0.002876$$

Solution of this equation gives two values of λ. The smaller (algebraic) value corresponds to operation at a negative angle of attack and can be ignored. The larger value, which corresponds to operation at a positive angle of attack, is

$$\lambda=-0.0050$$

With λ and θ_0 known, the calculation of the flapping angles is carried out with the help of tables I and II.

$$a_0=15[(0.1536)(-0.0050)+(0.1244)(0.0698)]-\frac{M_W}{I_1\Omega^2}$$
$$=\left(0.1187-\frac{M_W}{I_1\Omega^2}\right)\text{ radians}$$
$$a_1=(0.777)(-0.0050)+(1.041)(0.0698)$$
$$=0.0687\text{ radians}$$
$$b_1=15[(0.0721)(-0.0050)+(0.0591)(0.0698)]$$
$$-(0.452)\left(\frac{M_W}{I_1\Omega^2}\right)$$
$$=\left[(0.0563)-(0.452)\left(\frac{M_W}{I_1\Omega^2}\right)\right]\text{ radians}$$
$$a_2=(0.35)^2\left[\left(\frac{1.184+1.306}{2}\right)(-0.0050)\right.$$
$$\left.+\left(\frac{1.009+1.096}{2}\right)(0.0698)\right]$$
$$=0.0082\text{ radians}$$
$$b_2=(0.35)^2\left[\left(\frac{-0.314-0.354}{2}\right)(-0.0050)\right.$$
$$\left.+\left(\frac{-0.381-0.430}{2}\right)(0.0698)\right]$$
$$=-0.0033\text{ radians}$$

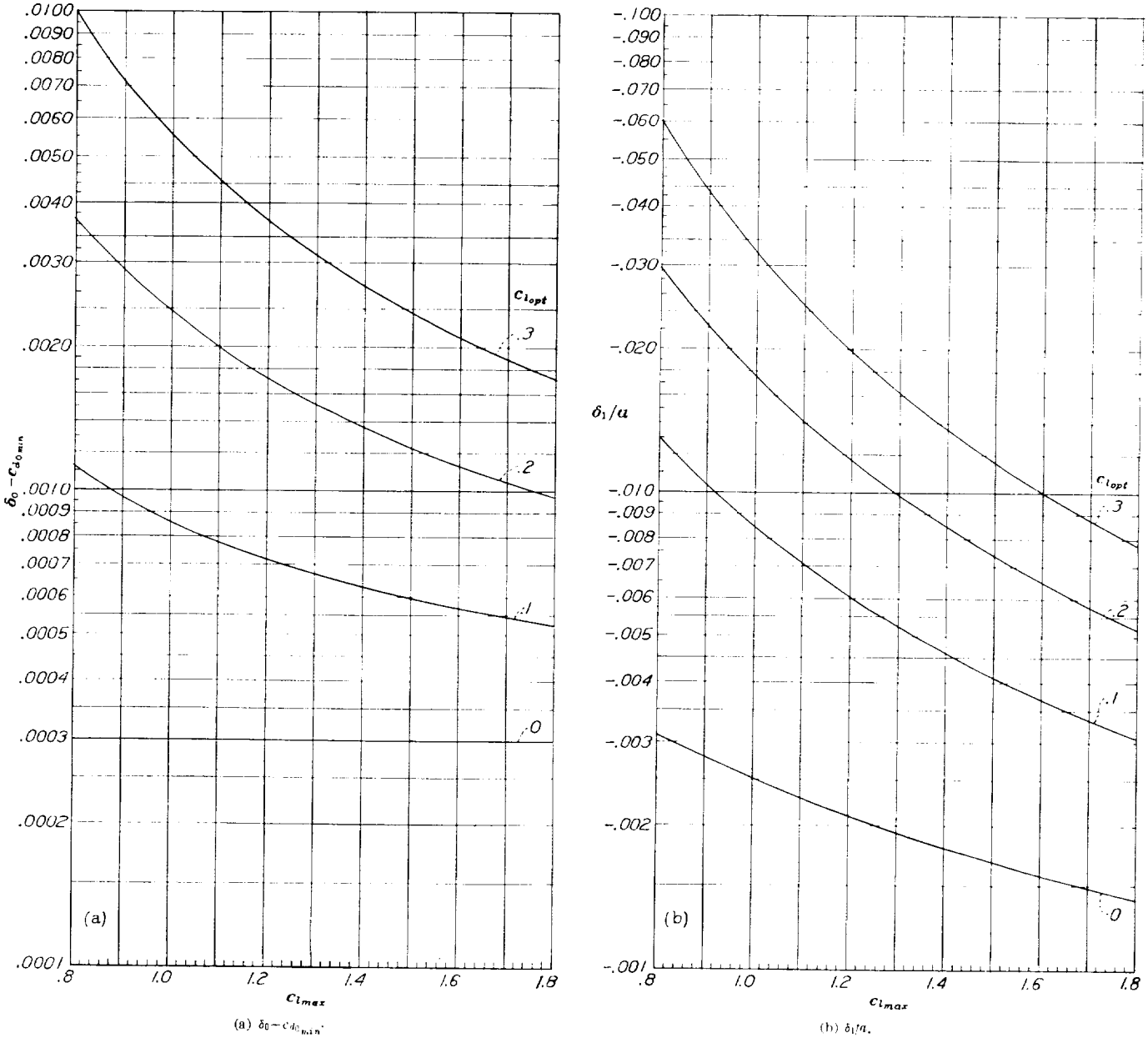

(a) $\delta_0 - c_{d_{0_{min}}}$. (b) δ_1/a.

FIGURE 2.—Charts for the determination of δ_0, δ_1, and δ_2 for different blade airfoil sections.

It is understood, of course, that the values of a_0, b_1, a_2, and b_2 depend on the value of the mass constant γ of the rotor. In these calculations, $\gamma = 15$ was used.

The thrust coefficient is obtained from equation (6) and table III

$$\frac{2C_T}{\sigma a} = (0.504)(-0.0050) + (0.361)(0.0698) = 0.0227$$

It will be shown later that the lift coefficient-solidity ratio C_L/σ is a particularly convenient parameter against which to plot the profile drag-lift ratio of rotors. This quantity is obtained on the assumption that $L = T \cos \alpha$ or

$$C_L \pi R^2 \frac{1}{2} \rho V^2 = C_T \rho \Omega^2 \pi R^4 \cos \alpha$$

from which

$$C_L = \frac{2C_T \cos \alpha}{\left(\frac{V}{\Omega R}\right)^2} = \frac{2C_T \cos^3 \alpha}{\mu^2}$$

and

$$\frac{C_L}{\sigma} = \frac{2C_T}{\sigma a} \frac{a \cos^3 \alpha}{\mu^2} \tag{24}$$

Ordinarily at tip-speed ratios above 0.15 or 0.20 the value of $\cos^3 \alpha$ can be taken as unity without serious error. Hence, in the present case

$$\frac{C_L}{\sigma} = (0.0227) \frac{5.73}{(0.35)^2} = 1.062$$

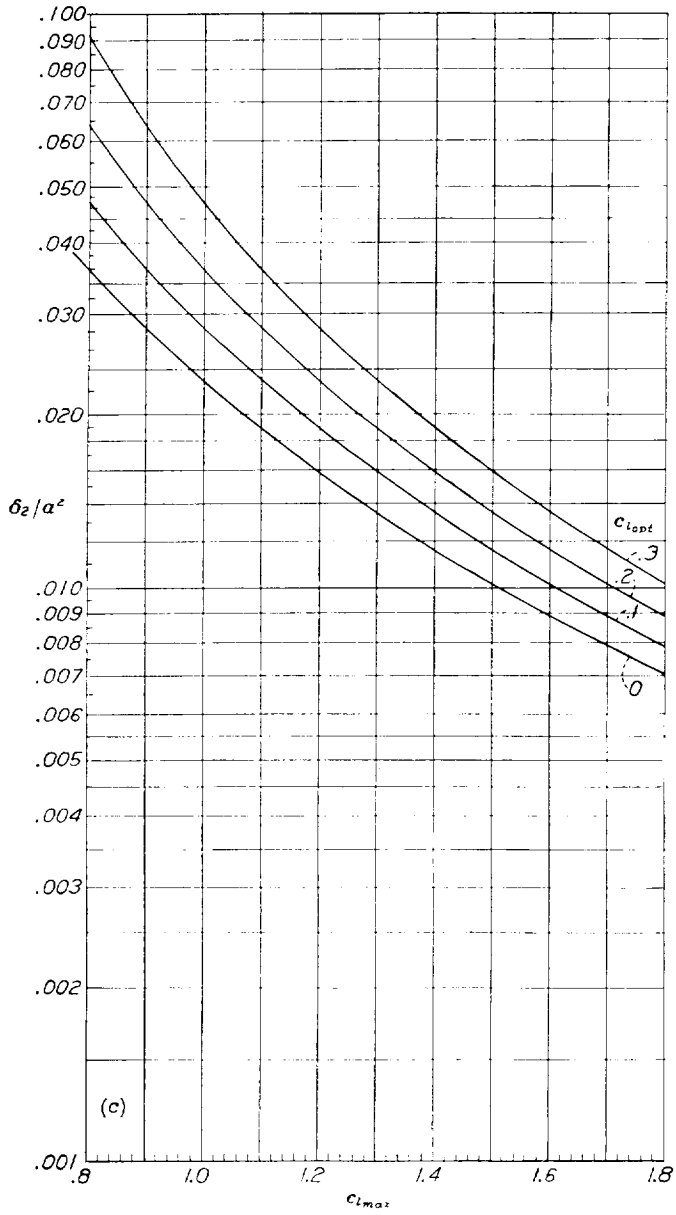

(c) δ_2/a^2.

The induced drag-lift ratio of a rotor, given by the second term of equation (11–4) of reference 1, is

$$\left(\frac{D}{L}\right)_i = \frac{\frac{1}{2}C_T}{\mu(\mu^2+\lambda^2)^{\frac{1}{2}}} \frac{1}{4}C_L \left\{ \frac{1}{\left[1+\left(\frac{\lambda}{\mu}\right)^2\right]^{\frac{1}{2}}} \cos^3\alpha \right\}$$

At tip-speed ratios above 0.15 the factor enclosed in the brace may be considered unity and

$$\left(\frac{D}{L}\right)_i = \frac{C_L}{\sigma} \times \frac{1}{4}\sigma \tag{25}$$

which is, in the present case,

$$1.062 \times \frac{\sigma}{4} = 0.266\sigma$$

The profile drag-lift ratio of the rotor is obtained from equations (13) and (14) and tables VI and VII:

$$\left(\frac{D}{L}\right)_0 [(0.1753)(-0.0050)+(0.1252)(0.0698)]$$
$$= \left(\frac{0.0087}{5.73}\right)(0.343)+\left(\frac{-0.0216}{5.73}\right)[(0.353)(-0.0050)$$
$$+(0.286)(0.0698)]+\left(\frac{0.400}{5.73}\right)[(0.627)(-0.0050)^2$$
$$+(0.930)(-0.0050)(0.0698)+(0.378)(0.0698)^2]$$

which gives

$$\left(\frac{D}{L}\right)_0 = 0.0711$$

EFFECT OF PITCH SETTING AND TIP-SPEED RATIO ON PROFILE DRAG-LIFT RATIO

The calculation of the profile drag-lift ratio of the autogiro rotor assumed in the preceding example has been repeated for a series of other combinations of the pitch angle θ_0 and the tip-speed ratio μ. The results are summarized by the chart shown in figure 3. This type of chart, in which profile drag-lift ratio is plotted against C_L/σ for various values of pitch and tip-speed ratio, is a particularly convenient method of presentation, in that the single chart completely specifies the lift and the drag characteristics of the rotor at any forward speed for all normal combinations of pitch, tip-speed ratio, and solidity.

LIMITS OF VALIDITY OF THEORY

It has been pointed out that the series used to approximate the profile-drag coefficient of the blade elements begins to underestimate seriously the drag coefficient when the parameter $(c_l - c_{l_{opt}})/(c_{l_{max}} - c_{l_{opt}})$ reaches a value of 0.8. The angle of attack of the blade element corresponding to this limiting condition is

$$\alpha_{r_{lim}} = \frac{0.8c_{l_{max}} + 0.2c_{l_{opt}}}{a} \tag{26}$$

Now, it is impossible to limit the application of the theory to flight conditions in which $\alpha_{r_{lim}}$ is never exceeded by any blade element. Whenever the rotor is in translation, some elements of the retreating blade will be operating at angles of attack above $\alpha_{r_{lim}}$. For moderate values of pitch and tip-speed ratio, however, these high values of the angle of attack are confined to parts of the rotor disk in which the square of the velocity of the air relative to the blade element is quite low. Under such conditions the total contribution of these blade elements to the rotor thrust, torque, and flapping is very small, and the error in its estimation is negligible.

As the tip-speed ratio or the pitch setting is increased, the high angle-of-attack region spreads to regions of

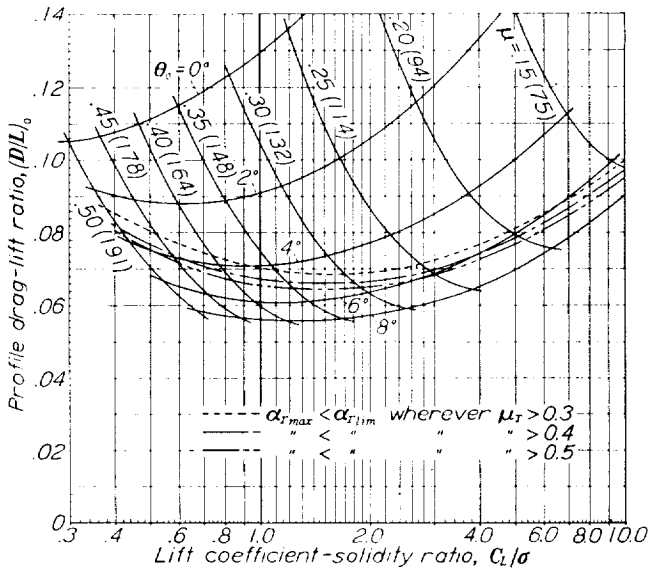

FIGURE 3.—Profile drag-lift ratio for sample rotor. The values in parentheses represent the forward speed in miles per hour at which the advancing blade tip reaches 75 percent of the speed of sound at sea level.

$$\text{Induced } \frac{D}{L} = \left(\frac{C_L}{\sigma}\right)\left(\frac{\sigma}{4}\right)$$

increasingly high velocity and the accuracy of the theory is correspondingly reduced. The extent to which the theory will be in error in any particular case will be approximately determined by the square of the maximum value of the tangential velocity component u_T at which elements reach the limiting angle of attack $\alpha_{r_{lim}}$. Hence, the rational interpretation of a chart such as the one shown in figure 3 requires the addition of a series of lines, each of which represents the locus of combinations of pitch and tip-speed ratio for which $\alpha_{r_{lim}}$ is the maximum angle of attack reached at the value of u_T specified for the line.

In order to construct the limiting lines just mentioned, it is necessary to derive a relation between the angle of attack of an element and its tangential-velocity component. The angle of attack is generally expressed by the formula

$$\alpha_r = \frac{u_P}{u_T} + \theta_0 + x\theta_1$$

or, after substitution for u_P from equation (9) of reference 2 and for x from equation (8) of reference 2,

$$\alpha_r = \theta_0 + \theta_1 u_T - \theta_1 \mu \sin\psi + b_1 \cos\psi - a_1 \sin\psi + 2b_2 \cos 2\psi - 2a_2 \sin 2\psi + \frac{1}{u_T}\left[\lambda + \mu a_1 + \left(-\mu a_0 + \frac{3}{2}\mu a_2\right)\cos\psi + \frac{3}{2}\mu b_2 \sin\psi - \frac{1}{2}\mu a_2 \cos 3\psi - \frac{1}{2}\mu b_2 \sin 3\psi\right] \quad (27)$$

This equation makes it possible to calculate the angle of attack corresponding to a specified tangential velocity u_T at all azimuth positions. It is not useful for the present purpose, however, until the azimuth angle ψ at which α_r becomes a maximum is determined. In a specific example, where numerical values of the flapping coefficients are available, the derivative of the expression can be equated to 0 and a numerical value can be obtained for ψ. This value of ψ, when substituted in the original expression, will determine the desired maximum value of α_r for the specified value of u_T. In general form, however, this method of solution results in expressions too complex for practical application, unless the rotor is assumed to have infinitely heavy blades.

For the rotor with infinitely heavy blades the mass constant γ and all flapping coefficients except a_1 are zero. Then

$$\alpha_r = \theta_0 + \theta_1 u_T - \theta_1 \mu \sin\psi - a_1 \sin\psi + \frac{\lambda}{u_T} + \frac{\mu a_1}{u_T}$$

The azimuth positions for maximum and minimum angles of attack are obtained from the condition that

$$\frac{d\alpha_r}{d\psi} = 0 = -\theta_1 \mu \cos\psi - a_1 \cos\psi$$

which gives $\psi = 90°$ for $\alpha_{r_{min}}$ and $\psi = 270°$ for $\alpha_{r_{max}}$. Substitution of $\psi = 270°$ gives

$$\alpha_{r_{max}} = \theta_0 + \theta_1(u_T + \mu) + \frac{\lambda}{u_T} + \left(1 + \frac{\mu}{u_T}\right)a_1$$

After substitution from equation (2),

$$\alpha_{r_{max}} = u_T\theta_1 + \lambda\left(\frac{2}{B^2\mu} + \frac{1}{2B^4\mu^3}\right) + \frac{\lambda}{u_T}\left(1 + \frac{2}{B^2\mu^2} + \frac{1}{2B^4\mu^4}\right) + \theta_0\left(1 + \frac{8}{3B^3\mu} + \frac{4}{3B^3\mu^3} + \frac{0.212}{B^4\mu^4}\right) + \frac{\theta_0}{u_T}\left(\frac{8}{3B^3\mu^2} + \frac{4}{3B^3\mu^4}\right) + \theta_1\left(3\mu + \frac{1}{B^2\mu^3}\right) + \frac{\theta_1}{u_T}\left(2\mu^2 + \frac{1}{B^2\mu^4}\right) \quad (28)$$

The coefficients of λ, λ/u_T, θ_0, θ_0/u_T, θ_1, and θ_1/u_T are given in table VIII.

TABLE VIII.—NUMERICAL VALUES OF THE COEFFICIENTS IN EQUATION (28) FOR $\alpha_{r_{max}}$

[$B = 0.97$]

Coefficient of \ Tip-speed ratio, μ	0.15	0.20	0.25	0.30	0.35	0.40	0.45	0.50
λ	0.321	0.430	0.540	0.653	0.768	0.886	1.008	1.133
λ/u_T	1.048	1.086	1.135	1.196	1.269	1.355	1.454	1.567
θ_0	1.418	1.562	1.711	1.866	2.028	2.199	2.380	2.572
θ_0/u_T	.063	.112	.178	.259	.359	.477	.617	.779
θ_1	.454	.608	.767	.929	1.096	1.268	1.447	1.633
θ_1/u_T	.046	.082	.129	.189	.261	.347	.449	.566

Under the conditions chosen for the illustrative example, $\theta_1=0$, $\theta_0=4°$, $\lambda=-0.0050$ and

$$\alpha_{r_{max}}=(-0.0050)\ (0.768)+\left(\frac{-0.0050}{u_T}\right)(1.269)$$
$$+(0.0698)\ (2.028)+\left(\frac{0.0698}{u_T}\right)(0.359)$$
$$=10.04°\text{ at }u_T=0.5$$

The maximum angle of attack does not reach a value as high as $(0.8c_{l_{max}}+0.2c_{l_{opt}})/a$ until u_T is as low as 0.279. Hence, the conditions chosen for the illustrative example lie within the range for which the theory may be expected to give reasonably accurate results.

The value of $\alpha_{r_{max}}$ has been calculated for all combinations of pitch and tip-speed ratio shown in figure 3 for values of u_T of 0.3, 0.4, and 0.5. For each of these three values of u_T, a series of combinations of θ_0 and μ at which $\alpha_{r_{max}}$ just reaches $(0.8c_{l_{max}}+0.2c_{l_{opt}})/a$ has been established by interpolation. Curves drawn through each series have been included in figure 3. At the present time it is not possible to estimate quantitatively the error in the theory corresponding to each of the three curves. Fortunately such an estimate is not absolutely essential. The rapidity of the growth, with pitch and tip-speed ratio, of the high angle-of-attack region beyond the line for $u_T=0.4$ makes this line a satisfactory limit in the present case.

A question naturally arises as to whether the fact that the blades are not infinitely heavy can be safely ignored in the determination of the limiting lines. In order to check on this point, three combinations of pitch and tip-speed ratio, for which $\alpha_{r_{max}}=\alpha_{r_{lim}}$ at $u_T=0.4$ for infinitely heavy blades, have been used with $u_T=0.4$ to calculate values of α_r against ψ directly from equation (27) when $\gamma=15$. The results are tabulated as follows:

μ	θ_0 (deg)	u_T	$\alpha_{r_{max}}$ (deg)	
			$\gamma=0$	$\gamma=15$
0.25	5.93	0.4	11.75	13.16
.35	4.82	.4	11.75	12.69
.45	3.93	.4	11.75	12.79

It is evident that the angles reach slightly higher values at a given u_T for blades of finite mass ($\gamma=15$). Hence, limit lines constructed on the assumption of $\gamma=0$ tend to overestimate slightly the range of conditions for which the theory is valid.

Up to this point the discussion has been concerned primarily with the determination of the limiting conditions of pitch and tip-speed ratio for which the theory can be expected to give accurate results. It should be pointed out, however, that the use of combinations of pitch and tip-speed ratio beyond these limits will result in an actual performance inferior to that predicted by the theory because of the drag of blade elements operating near and beyond the stall. The rapidity with which the high angles of attack spread to high velocities in the rotor under consideration indicates that the conditions of pitch and tip-speed ratio for optimum performance can be only slightly beyond the limits of accuracy of the theory.

EFFECT OF COMPRESSIBILITY ON ADVANCING BLADE

The speed at the tip of the advancing blade of a rotor in translation is

$$U=V+\Omega R$$

or, since $\mu=\frac{V}{\Omega R}$ approximately,

$$V=U\left(\frac{\mu}{\mu+1}\right) \tag{29}$$

The compressibility-shock wave usually forms on airfoil sections at between 75 and 80 percent of the speed of sound. Hence, the maximum speed at which a rotor can be flown without danger of loss in efficiency due to compressibility shock on the advancing blade tip may be considered to be

$$V_{max}=573\frac{\mu}{\mu+1}\text{ miles per hour} \tag{30}$$

Equation (30) indicates that the lines of constant tip-speed ratio on figure 3 are also lines of constant maximum permissible forward speed. For example, a rotor cannot fly at a forward speed greater than 148 miles per hour, at any value of C_L/σ to the right of the line $\mu=0.35$ in figure 3, without danger of compressibility shock on the advancing blade. Values of the maximum permissible speed, as given by equation (30), are noted for each tip-speed ratio on figure 3. It is apparent that, in the case of the constant-pitch autorotating rotor, the necessity of avoiding compressibility on the advancing blade restricts high-speed flight to inefficient combinations of pitch and tip-speed ratio.

CONCLUSIONS

1. Theoretically derived expressions for the thrust, the torque, and the profile drag-lift ratio of a lifting rotor in translation have been reduced to simple functions of the inflow velocity and the blade pitch. The various terms in these functions have coefficients that are functions of the tip-speed ratio but are, for practical purposes, independent of the mass constant. Values of these coefficients given in tables for specified values of the tip-speed ratio can be safely used to estimate the characteristics of any rotor of conventional design.

2. The relationship between the drag and the lift characteristics of an autorotating rotor, in forward flight at tip-speed ratios above 0.15, can be completely specified for various combinations of pitch, tip-speed ratio, and solidity by a single chart on which

the profile drag-lift ratio is plotted against the lift coefficient-solidity ratio for specified values of pitch and tip-speed ratio.

3. Beyond certain limiting combinations of pitch and tip-speed ratio, the excessive power required by blade elements operating at high speeds while near or beyond the stall adversely affects the over-all rotor performance to such an extent that the theoretical treatment is no longer accurate. By a method developed in the present paper it is possible to determine approximately these limiting combinations and thus to avoid the application of the theory to conditions in which the rotor performance would inevitably be overestimated.

4. The requirement that compressibility shock be avoided at the tip of the advancing blade restricts high-speed flight with an autorotating rotor to inefficient combinations of pitch and tip-speed ratio.

LANGLEY MEMORIAL AERONAUTICAL LABORATORY,
NATIONAL ADVISORY COMMITTEE FOR AERONAUTICS,
LANGLEY FIELD, VA., *March 17, 1941.*

APPENDIX

$$t_{1,1}=\frac{1}{6}B^3+0.040\mu^3-\frac{5}{144}\left(\frac{\gamma^2B^7}{144+\gamma^2B^8}\right)\mu^4$$

$$t_{1,2}=\frac{1}{8}B^4+\frac{1}{8}B^2\mu^2-\frac{1}{64}\mu^4-\frac{25}{576}\left(\frac{\gamma^2B^8}{144+\gamma^2B^8}\right)\mu^4$$

$$t_{1,3}=\frac{1}{10}B^5+\frac{1}{12}B^3\mu^2-\frac{1}{30}\left(\frac{\gamma^2B^9}{144+\gamma^2B^8}\right)\mu^4$$

$$t_{1,4}=\frac{2}{B^2}\mu+\frac{1}{2B^4}\mu^3+\frac{10}{27}\left(\frac{\gamma^2B^4}{144+\gamma^2B^8}\right)\mu^3$$

$$t_{1,5}=\frac{8}{3B}\mu+\frac{4}{3B^3}\mu^3+\frac{0.212}{B^4}\mu^4+\frac{25}{54}\left(\frac{\gamma^2B^5}{144+\gamma^2B^8}\right)\mu^3$$

$$t_{1,6}=2\mu+\frac{1}{B^2}\mu^3+\frac{16}{45}\left(\frac{\gamma^2B^6}{144+\gamma^2B^8}\right)\mu^3$$

$$t_{1,7}=\frac{2}{9}B^2\mu-\frac{1}{9}\mu^3+\frac{0.0767}{B}\mu^4+\frac{1}{144+\gamma^2B^8}\left(\frac{32}{3}+\frac{7}{162}\gamma^2B^8\right)\mu^3$$

$$t_{1,8}=\frac{1}{6}B^3\mu+\frac{1}{12}B\mu^3+0.0175\mu^4+\frac{1}{144+\gamma^2B^8}\left(\frac{92}{9}B+\frac{7}{216}\gamma^2B^9\right)\mu^3$$

$$t_{1,9}=\frac{2}{15}B^4\mu+\frac{2}{45}B^2\mu^3+0.0140B\mu^4+\frac{1}{144+\gamma^2B^8}\left(8B^2+\frac{7}{270}\gamma^2B^{10}\right)\mu^3$$

$$t_{1,10}=-\frac{4}{3B}\mu+\frac{2}{3B^3}\mu^3-\frac{0.140}{B^4}\mu^4$$

$$t_{2,1}=\frac{1}{144+\gamma^2B^8}\left(16\gamma B+\frac{7}{108}\gamma^3B^9\right)$$

$$t_{2,2}=\frac{1}{144+\gamma^2B^8}\left(\frac{46}{3}\gamma B^2+\frac{7}{144}\gamma^3B^{10}\right)$$

$$t_{2,3}=\frac{1}{144+\gamma^2B^8}\left(12\gamma B^3+\frac{7}{180}\gamma^3B^{11}\right)$$

$$t_{2,4}=-\frac{5}{9}\left(\frac{\gamma^2B^5}{144+\gamma^2B^8}\right)$$

$$t_{2,5}=-\frac{25}{36}\left(\frac{\gamma^2B^6}{144+\gamma^2B^8}\right)$$

$$t_{2,6}=-\frac{8}{15}\left(\frac{\gamma^2B^7}{144+\gamma^2B^8}\right)$$

$$t_{3,1}=\frac{1}{2}B^2+\frac{1}{4}\mu^2+\left[\frac{1}{4B^2}-\frac{5}{36}\left(\frac{\gamma^2B^6}{144+\gamma^2B^8}\right)\right]\mu^4$$

$$t_{3,2}=\frac{1}{3}B^3+\frac{1}{2}B\mu^2-\frac{4}{9\pi}\mu^3+\left[\frac{1}{3B}-\frac{25}{144}\left(\frac{\gamma^2B^7}{144+\gamma^2B^8}\right)\right]\mu^4$$

$$t_{3,3}=\frac{1}{4}B^4+\frac{1}{4}B^2\mu^2+\left[\frac{7}{32}-\frac{2}{15}\left(\frac{\gamma^2B^8}{144+\gamma^2B^8}\right)\right]\mu^4$$

$$t_{4,1}=\frac{1}{2}B^2+\left(\frac{5}{4}+\frac{1}{1296}\gamma^2B^8\right)\mu^2+\left[\frac{1}{2B^2}+\frac{\gamma^2B^6}{(144+\gamma^2B^8)^2}\left(\frac{4}{3}-\frac{37}{162}\gamma^2B^8-\frac{77}{46656}\gamma^4B^{16}\right)\right]\mu^4$$

$$t_{4,2}=\frac{1}{3}B^3+\left(\frac{8}{3}B+\frac{1}{864}\gamma^2B^9\right)\mu^2+\frac{2}{9\pi}\mu^3+\left[\frac{8}{3B}+\frac{\gamma^2B^7}{(144+\gamma^2B^8)^2}\left(\frac{224}{9}-\frac{11}{648}\gamma^2B^8-\frac{41}{31104}\gamma^4B^{16}\right)\right]\mu^4$$

$$t_{4,3}=-\frac{1}{4}B^4+\left(2B^2+\frac{1}{1080}\gamma^2B^{10}\right)\mu^2+\left[\frac{65}{32}+\frac{\gamma^2B^8}{(144+\gamma^2B^8)^2}\left(\frac{236}{15}-\frac{7}{108}\gamma^2B^8-\frac{47}{38880}\gamma^4B^{16}\right)\right]\mu^4$$

$$t_{4,4}=-\left(\frac{8}{9}B^2+\frac{1}{2304}\gamma^2B^{10}\right)\mu^2+\left[\frac{20}{9}+\frac{\gamma^2B^8}{(144+\gamma^2B^8)^2}\left(\frac{305}{36}+\frac{65}{1296}\gamma^2B^8-\frac{5}{82944}\gamma^4B^{16}\right)\right]\mu^4$$

$$t_{4,5}=-\left(\frac{4}{3}B^3+\frac{1}{1440}\gamma^2B^{11}\right)\mu^2+\left[\frac{10}{3}B+\frac{\gamma^2B^9}{(144+\gamma^2B^8)^2}\left(\frac{57}{5}+\frac{7}{144}\gamma^2B^8-\frac{11}{51840}\gamma^4B^{16}\right)\right]\mu^4$$

$$t_{4,6}=-\left(\frac{1}{2}B^4+\frac{1}{3600}\gamma^2B^{12}\right)\mu^2+\left[\frac{5}{4}B^2+\frac{\gamma^2B^{10}}{(144+\gamma^2B^8)^2}\left(\frac{92}{25}+\frac{1}{150}\gamma^2B^8-\frac{17}{129600}\gamma^4B^{16}\right)\right]\mu^4$$

$$t_{4,7}=-\frac{1}{108}B^5\mu^2+\frac{1}{144+\gamma^2B^8}\left(\frac{47}{9}B^3+\frac{7}{486}\gamma^2B^{11}\right)\mu^4$$

$$t_{4,8}=-\frac{1}{144}B^6\mu^2+\frac{1}{144+\gamma^2B^8}\left(\frac{485}{108}B^4+\frac{5}{1296}\gamma^2B^{12}\right)\mu^4$$

$$t_{4,9}=-\frac{1}{180}B^7\mu^2+\frac{1}{144+\gamma^2B^8}\left(\frac{18}{5}B^5+\frac{13}{3240}\gamma^2B^{13}\right)\mu^4$$

$$t_{4,10}=\frac{1}{36}B^2\mu^2+\frac{7}{144}\mu^4$$

$$t_{5,1}=\frac{1}{4}+\frac{1}{4}\mu^2-\frac{1}{32}\mu^4$$

$$t_{5,2}=\frac{1}{3}-\frac{5}{72}\left(\frac{\gamma^2B^5}{144+\gamma^2B^8}\right)\mu^4$$

$$t_{5,3}=\frac{1}{4}+\frac{1}{4}\mu^2-\frac{25}{288}\left(\frac{\gamma^2B^6}{144+\gamma^2B^8}\right)\mu^4$$

$$t_{5,4}=\frac{1}{5}+\frac{1}{6}\mu^2-\frac{1}{15}\left(\frac{\gamma^2B^7}{144+\gamma^2B^8}\right)\mu^4$$

$$t_{5,5}=\frac{1}{2}+\left[-\frac{1}{4}+\frac{1}{B^2}+\frac{1}{2B^4}+\gamma^2\left(\frac{1}{162}B^4-\frac{1}{81}B^5+\frac{1}{144}B^6\right)\right]\mu^2$$
$$+\left[-\frac{3}{4B^2}+\frac{1}{B^4}+\frac{1}{4B^6}+\gamma^2\left(-\frac{1}{162}B^2+\frac{1}{162}B^3+\frac{1}{324}B^4\right.\right.$$
$$\left.\left.-\frac{1}{576}B^6\right)+\frac{\gamma^2}{144+\gamma^2B^8}\left(\frac{7}{9}B^2-\frac{37}{27}B^3-\frac{13}{27}B^4\right)\right.$$
$$+\frac{\gamma^2}{(144+\gamma^2B^8)^2}(128B^2)+\frac{\gamma^4}{144+\gamma^2B^8}\left(\frac{7}{2916}B^{10}\right.$$
$$\left.-\frac{7}{1458}B^{11}-\frac{7}{2592}B^{12}\right)+\frac{\gamma^4}{(144+\gamma^2B^8)^2}\left(\frac{193}{162}B^{10}\right)$$
$$\left.+\frac{\gamma^6}{(144+\gamma^2B^8)^2}\left(\frac{49}{23328}B^{18}\right)\right]\mu^4$$

$$t_{5,6}=\frac{2}{3}+\left[\frac{4}{3B}+\frac{4}{3B^3}+\gamma^2\left(\frac{1}{108}B^5-\frac{1}{54}B^6+\frac{1}{96}B^7\right)\right]\mu^2+\frac{4}{9\pi}\mu^3$$
$$+\left[-\frac{1}{B}+\frac{8}{3B^3}+\frac{1}{B^5}+\gamma^2\left(-\frac{1}{108}B^4+\frac{13}{864}B^5-\frac{1}{384}B^7\right)\right.$$
$$+\frac{\gamma^2}{144+\gamma^2B^8}\left(\frac{161}{108}B^3-\frac{811}{324}B^4-\frac{113}{108}B^5\right)$$
$$+\frac{\gamma^2}{(144+\gamma^2B^8)^2}\left(\frac{736}{3}B^3\right)+\frac{\gamma^4}{144+\gamma^2B^8}\left(\frac{7}{1944}B^{11}\right.$$
$$\left.-\frac{7}{972}B^{12}-\frac{7}{1728}B^{13}\right)+\frac{\gamma^4}{(144+\gamma^2B^8)^2}\left(\frac{233}{108}B^{11}\right)$$
$$\left.+\frac{\gamma^6}{(144+\gamma^2B^8)^2}\left(\frac{49}{15552}B^{19}\right)\right]\mu^4$$

$$t_{5,7}=\frac{1}{2}+\left[1+\frac{1}{B^2}+\gamma^2\left(\frac{1}{135}B^6-\frac{2}{135}B^7+\frac{1}{120}B^8\right)\right]\mu^2$$
$$+\left[-\frac{11}{16}+\frac{2}{B^2}+\frac{3}{4B^4}\right.$$
$$+\gamma^2\left(-\frac{1}{810}B^4-\frac{2}{405}B^5+\frac{23}{2160}B^6-\frac{1}{480}B^8\right)$$
$$+\frac{\gamma^2}{144+\gamma^2B^8}\left(\frac{157}{135}B^4-\frac{37}{18}B^5-\frac{13}{18}B^6\right)$$
$$+\frac{\gamma^2}{(144+\gamma^2B^8)^2}(192B^4)$$
$$+\frac{\gamma^4}{144+\gamma^2B^8}\left(\frac{7}{2430}B^{12}-\frac{7}{1215}B^{13}-\frac{7}{2160}B^{14}\right)$$
$$+\frac{\gamma^4}{(144+\gamma^2B^8)^2}\left(\frac{229}{135}B^{12}\right)$$
$$\left.+\frac{\gamma^6}{(144+\gamma^2B^8)^2}\left(\frac{49}{19440}B^{20}\right)\right]\mu^4$$

$$t_{5,8}=\frac{1}{4}+\left[\frac{1}{4}+\frac{8}{9B^2}+\gamma^2\left(\frac{1}{288}B^6-\frac{1}{144}B^7+\frac{1}{256}B^8\right)\right]\mu^2$$
$$+\left[-\frac{1}{32}+\frac{4}{3B^2}+\frac{8}{9B^4}\right.$$
$$+\gamma^2\left(\frac{1}{288}B^4-\frac{1}{96}B^5+\frac{11}{1152}B^6-\frac{1}{1024}B^8\right)$$
$$+\frac{\gamma^2}{144+\gamma^2B^8}\left(\frac{119}{162}B^4-\frac{94}{81}B^5-\frac{47}{72}B^6\right)$$
$$+\frac{\gamma^2}{(144+\gamma^2B^8)^2}\left(\frac{1058}{9}B^4\right)$$
$$+\frac{\gamma^4}{144+\gamma^2B^8}\left(\frac{7}{5184}B^{12}-\frac{7}{2592}B^{13}-\frac{7}{4608}B^{14}\right)$$
$$+\frac{\gamma^4}{(144+\gamma^2B^8)^2}\left(\frac{2557}{2592}B^{12}\right)$$
$$\left.+\frac{\gamma^6}{(144+\gamma^2B^8)^2}\left(\frac{49}{41472}B^{20}\right)\right]\mu^4$$

$$t_{5,9}=\frac{2}{5}+\left[\frac{1}{3}+\frac{4}{3B}+\gamma^2\left(\frac{1}{180}B^7-\frac{1}{90}B^8+\frac{1}{160}B^9\right)\right]\mu^2$$
$$+\left[\frac{4}{3B^3}+\frac{2}{B}+\gamma^2\left(\frac{1}{216}B^5-\frac{2}{135}B^6+\frac{41}{2880}B^7-\frac{1}{640}B^9\right)\right.$$
$$+\frac{\gamma^2}{144+\gamma^2B^8}\left(\frac{617}{540}B^5-\frac{2087}{1080}B^6-\frac{107}{120}B^7\right)$$
$$+\frac{\gamma^2}{(144+\gamma^2B^8)^2}(184B^5)$$
$$+\frac{\gamma^4}{144+\gamma^2B^8}\left(\frac{7}{3240}B^{13}-\frac{7}{1620}B^{14}-\frac{7}{2880}B^{15}\right)$$
$$+\frac{\gamma^4}{(144+\gamma^2B^8)^2}\left(\frac{31}{20}B^{13}\right)$$
$$\left.+\frac{\gamma^6}{(144+\gamma^2B^8)^2}\left(\frac{49}{25920}B^{21}\right)\right]\mu^4$$

$$t_{5,10}=\frac{1}{6}+\left[\frac{5}{8}+\gamma^2\left(\frac{1}{450}B^8-\frac{1}{225}B^9+\frac{1}{400}B^{10}\right)\right]\mu^2+\left[\frac{1}{2B^2}+\frac{3}{4}\right.$$
$$+\gamma^2\left(\frac{1}{675}B^6-\frac{7}{1350}B^7+\frac{19}{3600}B^8-\frac{1}{1600}B^{10}\right)$$
$$+\frac{\gamma^2}{144+\gamma^2B^8}\left(\frac{4}{9}B^6-\frac{4}{5}B^7-\frac{3}{10}B^8\right)$$
$$+\frac{\gamma^2}{(144+\gamma^2B^8)^2}(72B^6)$$
$$+\frac{\gamma^4}{144+\gamma^2B^8}\left(\frac{7}{8100}B^{14}-\frac{7}{4050}B^{15}-\frac{7}{5400}B^{16}\right)$$
$$+\frac{\gamma^4}{(144+\gamma^2B^8)^2}\left(\frac{137}{225}B^{14}\right)$$
$$\left.+\frac{\gamma^6}{(144+\gamma^2B^8)^2}\left(\frac{49}{64800}B^{22}\right)\right]\mu^4$$

$$t_{5,11}=\left(-\frac{2}{27}B+\frac{4}{27}B^2-\frac{1}{12}B^3\right)\mu^2+\left[\frac{2}{27B}-\frac{2}{27}-\frac{1}{27}B+\frac{1}{48}B^3\right.$$
$$+\frac{1}{144+\gamma^2B^8}\left(-\frac{32}{9B}+\frac{64}{9}+4B\right)$$
$$\left.+\frac{\gamma^2}{144+\gamma^2B^8}\left(-\frac{7}{486}B^7+\frac{7}{243}B^8+\frac{7}{432}B^9\right)\right]\mu^4$$

$$t_{5,12}=\left(-\frac{1}{18}B^2+\frac{1}{9}B^3-\frac{1}{16}B^4\right)\mu^2+\left[\frac{1}{18}B-\frac{13}{144}B^2+\frac{1}{64}B^4\right.$$
$$+\frac{1}{144+\gamma^2B^8}\left(-\frac{92}{27}+\frac{184}{27}B+\frac{23}{6}B^2\right)$$
$$\left.+\frac{\gamma^2}{144+\gamma^2B^8}\left(-\frac{7}{648}B^8+\frac{7}{324}B^9+\frac{7}{576}B^{10}\right)\right]\mu^4$$

$$t_{5,13}=\left(-\frac{2}{45}B^3+\frac{4}{45}B^4-\frac{1}{20}B^5\right)\mu^2+\left[\frac{1}{135}B+\frac{4}{135}B^2-\frac{23}{360}B^3+\frac{1}{80}B^5+\frac{1}{144+\gamma^2B^8}\left(-\frac{8}{3}B+\frac{16}{3}B^2+3B^3\right)+\frac{\gamma^2}{144+\gamma^2B^8}\left(-\frac{7}{810}B^9+\frac{7}{405}B^{10}+\frac{7}{720}B^{11}\right)\right]\mu^4$$

$$t_{5,14}=\left(\frac{1}{4}-\frac{4}{9B}+\frac{2}{9B^2}\right)\mu^2+\left(-\frac{1}{16}+\frac{1}{9B^2}+\frac{2}{9B^3}-\frac{2}{9B^4}\right)\mu^4$$

$$t_{6,1}=\frac{1}{4}+\frac{3}{4}\mu^2+\frac{3}{32}\mu^4$$

$$t_{6,2}=\frac{1}{3}+\left(\frac{1}{2}-\frac{1}{3B^2}\right)\mu^2+\left(\frac{1}{4B^2}-\frac{1}{12B^4}\right)\mu^4-\frac{5}{81}\left(\frac{\gamma^2B^4}{144+\gamma^2B^8}\right)\mu^4$$

$$t_{6,3}=\frac{1}{4}+\left(\frac{3}{4}-\frac{4}{9B}\right)\mu^2+\left(\frac{1}{3B}-\frac{2}{9B^3}\right)\mu^4-\frac{25}{324}\left(\frac{\gamma^2B^8}{144+\gamma^2B^8}\right)\mu^4$$

$$t_{6,4}=\frac{1}{5}+\frac{1}{6}\mu^2+\left(\frac{1}{4}-\frac{1}{6B^2}\right)\mu^4-\frac{8}{135}\left(\frac{\gamma^2B^6}{144+\gamma^2B^8}\right)\mu^4$$

$$t_{6,5}=\frac{1}{2}+\left[\frac{1}{4}+\frac{1}{2B^4}+\gamma^2\left(\frac{1}{162}B^4-\frac{1}{81}B^5+\frac{1}{144}B^6\right)\right]\mu^2+\left[\frac{1}{2B^2}+\frac{1}{4B^4}+\frac{1}{4B^6}+\gamma^2\left(-\frac{1}{162}B^2+\frac{1}{162}B^3+\frac{1}{108}B^4-\frac{1}{108}B^5+\frac{1}{576}B^6\right)+\frac{\gamma^2}{144+\gamma^2B^8}\left(\frac{7}{9}B^2-\frac{79}{27}B^3+\frac{2}{3}B^4-\frac{5}{18}B^5\right)+\frac{\gamma^2}{(144+\gamma^2B^8)^2}\left(128B^2\right)+\frac{\gamma^4}{144+\gamma^2B^8}\left(\frac{7}{2916}B^{10}-\frac{7}{729}B^{11}+\frac{7}{2592}B^{12}\right)+\frac{\gamma^4}{(144+\gamma^2B^8)^2}\left(\frac{193}{162}B^{10}\right)+\frac{\gamma^6}{(144+\gamma^2B^8)^2}\left(\frac{49}{23328}B^{18}\right)\right]\mu^4$$

$$t_{6,6}=\frac{2}{3}+\left[1-\frac{2}{3B^2}+\frac{4}{3B^3}+\gamma^2\left(\frac{1}{108}B^5-\frac{1}{54}B^6+\frac{1}{96}B^7\right)\right]\mu^2-\frac{8}{9\pi}\mu^3+\left[\frac{2}{3B}+\frac{1}{2B^2}+\frac{2}{3B^3}-\frac{1}{6B^4}+\frac{1}{B^5}+\gamma^2\left(-\frac{1}{108}B^4+\frac{7}{288}B^5-\frac{1}{72}B^6+\frac{1}{384}B^7\right)+\frac{\gamma^2}{144+\gamma^2B^8}\left(\frac{161}{108}B^3-\frac{1817}{324}B^4+\frac{41}{36}B^5-\frac{25}{72}B^6\right)+\frac{\gamma^2}{(144+\gamma^2B^8)^2}\left(\frac{736}{3}B^3\right)+\frac{\gamma^4}{144+\gamma^2B^8}\left(\frac{7}{1944}B^{11}-\frac{7}{486}B^{12}+\frac{7}{1728}B^{13}\right)+\frac{\gamma^4}{(144+\gamma^2B^8)^2}\left(\frac{233}{108}B^{11}\right)+\frac{\gamma^6}{(144+\gamma^2B^8)^2}\left(\frac{49}{15552}B^{19}\right)\right]\mu^4$$

$$t_{6,7}=\frac{1}{2}+\left[\frac{1}{2}+\frac{1}{2B^2}+\gamma^2\left(\frac{1}{135}B^6-\frac{2}{135}B^7+\frac{1}{120}B^8\right)\right]\mu^2+\left[\frac{7}{16}+\frac{3}{4B^2}+\frac{5}{8B^4}+\gamma^2\left(-\frac{1}{810}B^4-\frac{2}{405}B^5+\frac{13}{720}B^6-\frac{1}{90}B^7+\frac{1}{480}B^8\right)+\frac{\gamma^2}{144+\gamma^2B^8}\left(\frac{289}{270}B^4+\frac{193}{45}B^5+\frac{9}{10}B^6-\frac{4}{15}B^7\right)+\frac{\gamma^2}{(144+\gamma^2B^8)^2}(192B^4)+\frac{\gamma^4}{144+\gamma^2B^8}\left(\frac{7}{2430}B^{12}-\frac{14}{1215}B^{13}+\frac{7}{2160}B^{14}\right)+\frac{\gamma^4}{(144+\gamma^2B^8)^2}\left(\frac{229}{135}B^{12}\right)+\frac{\gamma^6}{(144+\gamma^2B^8)^2}\left(\frac{49}{19440}B^{20}\right)\right]\mu^4$$

$$t_{6,8}=\frac{1}{4}+\left[\frac{3}{4}-\frac{8}{9B}+\frac{8}{9B^2}+\gamma^2\left(\frac{1}{288}B^6-\frac{1}{144}B^7+\frac{1}{256}B^8\right)\right]\mu^2+\left[\frac{3}{32}+\frac{2}{3B}+\frac{4}{9B^2}-\frac{4}{9B^3}+\frac{8}{9B^4}+\gamma^2\left(\frac{1}{288}B^4-\frac{1}{96}B^5+\frac{5}{384}B^6-\frac{1}{192}B^7+\frac{1}{1024}B^8\right)+\frac{\gamma^2}{144+\gamma^2B^8}\left(\frac{119}{162}B^4-\frac{451}{162}B^5+\frac{23}{48}B^6\right)+\frac{\gamma^2}{(144+\gamma^2B^8)^2}\left(\frac{1058}{9}B^4\right)+\frac{\gamma^4}{144+\gamma^2B^8}\left(\frac{7}{5184}B^{12}-\frac{7}{1296}B^{13}+\frac{7}{4608}B^{14}\right)+\frac{\gamma^4}{(144+\gamma^2B^8)^2}\left(\frac{2557}{2592}B^{12}\right)+\frac{\gamma^6}{(144+\gamma^2B^8)^2}\left(\frac{49}{41472}B^{20}\right)\right]\mu^4$$

$$t_{6,9}=\frac{2}{5}+\left[1-\frac{2}{3}+\frac{2}{3B}+\gamma^2\left(\frac{1}{180}B^7-\frac{1}{90}B^8+\frac{1}{160}B^9\right)\right]\mu^2+\left[\frac{1}{2}+\frac{1}{B}-\frac{1}{3B^2}+\frac{1}{B^3}+\gamma^2\left(\frac{1}{216}B^5-\frac{2}{135}B^6+\frac{19}{960}B^7-\frac{1}{120}B^8+\frac{1}{640}B^9\right)+\frac{\gamma^2}{144+\gamma^2B^8}\left(\frac{1109}{1080}B^5-\frac{2279}{540}B^6+\frac{91}{120}B^7\right)+\frac{\gamma^2}{(144+\gamma^2B^8)^2}(184B^5)+\frac{\gamma^4}{144+\gamma^2B^8}\left(\frac{7}{3240}B^{13}-\frac{7}{810}B^{14}+\frac{7}{2880}B^{15}\right)+\frac{\gamma^4}{(144+\gamma^2B^8)^2}\left(\frac{31}{20}B^{13}\right)+\frac{\gamma^6}{(144+\gamma^2B^8)^2}\left(\frac{49}{25920}B^{21}\right)\right]\mu^4$$

$$t_{6,10}=\frac{1}{6}+\left[\frac{3}{8}+\gamma^2\left(\frac{1}{450}B^8-\frac{1}{225}B^9+\frac{1}{400}B^{10}\right)\right]\mu^2+\left[\frac{1}{2}+\frac{1}{4B^2}+\gamma^2\left(\frac{1}{675}B^6-\frac{7}{1350}B^7+\frac{3}{400}B^8-\frac{1}{300}B^9+\frac{1}{1600}B^{10}\right)+\frac{\gamma^2}{144+\gamma^2B^8}\left(\frac{16}{45}B^6-\frac{8}{5}B^7+\frac{3}{10}B^8\right)+\frac{\gamma^2}{(144+\gamma^2B^8)^2}(72B^6)+\frac{\gamma^4}{144+\gamma^2B^8}\left(\frac{7}{8100}B^{14}-\frac{7}{2025}B^{15}+\frac{7}{7200}B^{16}\right)+\frac{\gamma^4}{(144+\gamma^2B^8)^2}\left(\frac{137}{225}B^{14}\right)+\frac{\gamma^6}{(144+\gamma^2B^8)^2}\left(\frac{49}{64800}B^{22}\right)\right]\mu^4$$

$$t_{6,11}=\left(-\frac{2}{27}B+\frac{4}{27}B^2-\frac{1}{12}B^3\right)\mu^2+\left[\frac{2}{27}B-\frac{2}{27}-\frac{1}{9}B+\frac{1}{9}B^2-\frac{1}{48}B^3+\frac{1}{144+\gamma^2B^8}\left(-\frac{32}{9B}+\frac{128}{9}-4B\right)+\frac{\gamma^2}{144+\gamma^2B^8}\left(-\frac{7}{486}B^7+\frac{14}{243}B^8-\frac{7}{432}B^9\right)\right]\mu^4$$

$$t_{6,12}=\left(-\frac{1}{18}B^2+\frac{1}{9}B^3-\frac{1}{16}B^4\right)\mu^2+\left[\frac{1}{18}B-\frac{7}{48}B^2+\frac{1}{12}B^3-\frac{1}{64}B^4+\frac{1}{144+\gamma^2B^8}\left(-\frac{92}{27}+\frac{368}{27}B-\frac{23}{6}B^2\right)+\frac{\gamma^2}{144+\gamma^2B^8}\left(-\frac{7}{648}B^8+\frac{7}{162}B^9-\frac{7}{576}B^{10}\right)\right]\mu^4$$

$$t_{6,13}=\left(-\frac{2}{45}B^3+\frac{4}{45}B^4-\frac{1}{20}B^5\right)\mu^2+\left[\frac{1}{135}B+\frac{4}{135}B^2-\frac{13}{120}B^3+\frac{1}{15}B^4-\frac{1}{80}B^5+\frac{1}{144+\gamma^2B^8}\left(-\frac{8}{3}B+\frac{32}{3}B^2-3B^3\right)+\frac{\gamma^2}{144+\gamma^2B^8}\left(-\frac{7}{810}B^9+\frac{14}{405}B^{10}-\frac{7}{720}B^{11}\right)\right]\mu^4$$

$$t_{6,14}=\left(\frac{2}{9B^2}-\frac{4}{9B}+\frac{1}{4}\right)\mu^2+\left(-\frac{2}{9B^4}+\frac{2}{9B^3}+\frac{1}{3B^2}-\frac{1}{3B}+\frac{1}{16}\right)\mu^4$$

REFERENCES

1. Wheatley, John B.: An Aerodynamic Analysis of the Autogiro Rotor with a Comparison between Calculated and Experimental Results. Rep. No. 487, NACA, 1934.
2. Wheatley, John B.: An Analytical and Experimental Study of the Effect of Periodic Blade Twist on the Thrust, Torque, and Flapping Motion of an Autogiro Rotor. Rep. No. 591, NACA, 1937.
3. Sissingh, G.: Contribution to the Aerodynamics of Rotating-Wing Aircraft. T. M. No. 921, NACA, 1939.
4. Jacobs, Eastman N., and Sherman, Albert: Airfoil Section Characteristics as Affected by Variations of the Reynolds Number. Rep. No. 586, NACA, 1937.
5. Bailey, F. J., Jr.: A Study of the Torque Equilibrium of an Autogiro Rotor. Rep. No. 623, NACA, 1938.
6. Jacobs, Eastman N., and Abbott, Ira H.: Airfoil Section Data Obtained in the N. A. C. A. Variable-Density Tunnel as Affected by Support Interference and Other Corrections. Rep. No. 669, NACA, 1939.
7. Bicknell, Joseph: Determination of the Profile Drag of an Airplane Wing in Flight at High Reynolds Numbers. Rep. No. 667, NACA, 1939.